the plant journal

SEB Society for Experimental Biology

The Plant Journal (2019) **98,** 1060–1077 doi: 10.1111/tpj.14302

Multiomics analysis reveals a distinct mechanism of oleaginousness in the emerging model alga *Chromochloris zofingiensis*

Jin Liu*[,1], Zheng Sun[2], Xuemei Mao[1], Henri Gerken[3], Xiaofei Wang[1] and Wenqiang Yang[4]

[1]*Laboratory for Algae Biotechnology & Innovation, College of Engineering, Peking University, Beijing 100871, China,*

[2]*International Research Center for Marine Biosciences, Ministry of Science and Technology, Shanghai Ocean University, Shanghai 201306, China,*

[3]*School of Sustainable Engineering and the Built Environment, Arizona State University Polytechnic campus, Mesa, AZ, 85212, USA, and*

[4]*Photosynthesis Research Center, Key Laboratory of Photobiology, Institute of Botany, Chinese Academy of Sciences, Beijing 100093, China*

Received 30 October 2018; revised 15 February 2019; accepted 19 February 2019; published online 3 March 2019.
*For correspondence (e-mail gjinliu@pku.edu.cn)

SUMMARY

***Chromochloris zofingiensis*, featured due to its capability to simultaneously synthesize triacylglycerol (TAG) and astaxanthin, is emerging as a leading candidate alga for production uses. To better understand the oleaginous mechanism of this alga, we conducted a multiomics analysis by systematically integrating time-resolved transcriptomes, lipidomes and metabolomes in response to nitrogen deprivation. The data analysis unraveled the distinct mechanism of TAG accumulation, which involved coordinated stimulation of multiple biological processes including supply of energy and reductants, carbon reallocation from protein and starch, and 'pushing' and 'pulling' carbon to TAG synthesis. Unlike the model alga *Chlamydomonas*, *de novo* fatty acid synthesis in *C. zofingiensis* was promoted, together with enhanced turnover of both glycolipids and phospholipids, supporting the drastic need of acyls for TAG assembly. Moreover, genomewide analysis identified many key functional enzymes and transcription factors that had engineering potential for TAG modulation. Two genes encoding glycerol-3-phosphate acyltransferase (GPAT), the first committed enzyme for TAG assembly, were found in the *C. zofingiensis* genome; *in vivo* functional characterization revealed that extrachloroplastic GPAT instead of chloroplastic GPAT played a central role in TAG synthesis. These findings illuminate distinct oleaginousness mechanisms in *C. zofingiensis* and pave the way towards rational manipulation of this alga to become an emerging model for trait improvements.**

Keywords: *Chromochloris zofingiensis*, glycerol-3-phosphate acyltransferase, oleaginousness, multiomics, trait improvement, triacylglycerol.

INTRODUCTION

Algae-derived lipids, possessing substantial advantages over plant oils for biofuel production, have been considered as the next-generation biodiesel feedstock capable of meeting the existing demand for transportation fuels (Chisti, 2007; Hu *et al.*, 2008; Wijffels and Barbosa, 2010). Past decades have witnessed significant progress in the exploration of algae for biodiesel production, including alga selection, strain trait improvement, development of state-of-the-art cultivation technologies with flue gas and/or wastewater treatment and optimization of downstream processes (Lenka *et al.*, 2016; Zhou *et al.*, 2017; Raheem *et al.*, 2018). Nevertheless, challenges remain yet to be addressed to achieve cost-effective production of algae-based biodiesel (Chisti, 2013; Rodionova *et al.*, 2017). Producing lipids with value-added products in an integrated way represents an emerging research direction to offset the production cost of algal biodiesel.

Chromochloris zofingiensis, a freshwater green alga, also referred to as *Chlorella zofingiensis* or *Muriella zofingiensis*, is able to grow robustly to high cell densities under multitrophic conditions (Del Campo *et al.*, 2004; Ip *et al.*, 2004; Sun *et al.*, 2008; Liu *et al.*, 2013; Mulders *et al.*, 2014). The capacity for accumulating high levels of triacylglycerol (TAG), the most energy-dense lipid, has made

C. zofingiensis a promising feedstock for biodiesel production (Liu *et al.*, 2010, 2011, 2016a; Mulders *et al.*, 2014). *C. zofingiensis* has also been cited as a potential alternative to *Haematococcus pluvialis* for producing astaxanthin (Liu *et al.*, 2014a), a high-value keto-carotenoid with strong anti-oxidative activity and broad industrial applications (Fraser and Bramley, 2004; Ambati *et al.*, 2014). The characteristic that TAG and astaxanthin can be triggered to accumulate simultaneously, under conditions such as high carbon/nitrogen ratio, nitrogen deprivation (ND) and/or high light (HL) (Liu *et al.*, 2012a, 2016a; Mulders *et al.*, 2014), makes *C. zofingiensis* a leading candidate for future commercial production. Efforts have been made mainly via the optimization of culture conditions to enhance *C. zofingiensis* production (Liu *et al.*, 2010, 2012a, 2016a; Mulders *et al.*, 2014). However, improvements through genetic engineering are still needed to maximize the content and yield of TAG. These will rely on a global understanding of the biology and molecular regulation of oleaginousness in *C. zofingiensis* that had not been possible before the *C. zofingiensis* genome was recently sequenced and released (Roth *et al.*, 2017).

As in higher plants, algal TAG biosynthesis is mediated mainly via two pathways, an acyl-CoA-dependent Kennedy pathway and an acyl-CoA-independent pathway (Merchant *et al.*, 2012; Li-Beisson *et al.*, 2015). The former route is believed to contribute predominantly to abiotic stress-associated TAG assembly, which employs acyl-CoAs as the acyl donor and involves a series of acylation steps. Diacylglycerol acyltransferase (DGAT), responsible for the last acylation step of TAG synthesis, has been well studied in algae (Sanjaya *et al.*, 2013; Iwai *et al.*, 2014; Liu *et al.*, 2016b; Wei *et al.*, 2017; Xin *et al.*, 2017; Zienkiewicz *et al.*, 2017). By contrast, glycerol-3-phosphate acyltransferase (GPAT) that catalyzes the first acylation step is rarely touched for functional characterization in algae. Multiple biological pathways are likely to be involved to support TAG assembly and accumulation, including central carbon metabolism, fatty acid synthesis, membrane lipids turnover and input of energy and reductants, which has been suggested for the model alga *Chlamydomonas reinhardtii* (Goodenough *et al.*, 2014) and the marine alga *Nannochloropsis oceanica* (Li *et al.*, 2014), although the two algae possess key distinctions. Because of its unique properties, established transformation systems and annotated genome (Liu *et al.*, 2014a,b; Roth *et al.*, 2017), *C. zofingiensis* is emerging as a model alga for fundamental study. Nevertheless, the mechanism of oleaginousness has been rarely investigated for the alga and remains largely unknown.

To fill the gap, here we generated time-resolved transcriptomes via large-scale RNA-seq and determined the time-course profiles of lipids and other compounds for photoautotrophic *C. zofingiensis* cells upon ND, an efficient inducer for TAG accumulation. The congruent analysis of these 'omics data correlating gene expression with metabolite dynamics, plus the functional characterization of GPATs, on the one hand elucidated physiological pathways and key enzymes for lipid metabolism and, on the other hand, identified several global regulators potentially controlling TAG accumulation. These findings not only help us better understand the molecular mechanisms of algal TAG biosynthesis, but also facilitate future manipulation through rational genetic engineering for trait improvements in this alga and perhaps other industrially relevant species/strains.

RESULTS AND DISCUSSION

Biochemical variations in response to nitrogen deprivation

We performed a time-resolved analysis of cellular compounds including protein, starch and lipids in response to ND (Figure 1 and Table S1). Upon ND, the protein exhibited an immediate drop, while starch showed no decrease up to 48 h of ND; by contrast, lipid increased gradually. Triacylglycerol (TAG), the highest energy-dense neutral lipid class, showed a rapid and drastic increase (23-fold at 96 h), accompanied by the drop of membrane lipids to different extents. Fatty acids were induced by ND as well, with C18:1 having the highest increase (eight-fold at 96 h).

In addition, a comparative metabolomics analysis was conducted for 0 and 12 h of ND: 145 metabolites were detected and quantified as relative values of ND12/ND0 (Table S2). In response to ND, 60 metabolites (41%) changed significantly in abundance, of which 40 showed an increase and 20 showed a decrease. Specifically, the metabolites that decreased in their abundance upon ND were enriched in amino acid and nucleotide metabolism as well as in the TCA cycle, while the metabolites that increased upon ND had no specific enrichment.

Global gene expression analysis

To investigate the molecular mechanisms of lipogenesis in parallel with biochemical variation in *C. zofingiensis*, global gene expression as a function of time upon ND was measured by RNA-seq. Considering that the changes in gene expression upon ND may precede the changes in cellular compounds, the time points 0, 3, 6, 12 and 24 h were chosen for culture sampling and RNA-seq, with three biological replicates for each time point. Fifteen high-quality transcript profiles (Table S3) were generated with high reproducibility among the three biological replicates for each time point (Pearson correlation > 0.94; Figure S1). Furthermore, the time-resolved transcriptomes were validated by quantitative real-time PCR (qPCR) analysis of 12 genes, with the coefficient being 0.89 (R^2) (Figure S2 and Table S4). In total, 14 309 genes, representing 93.7% of the annotated genes in the *C. zofingiensis* genome (Roth *et al.*,

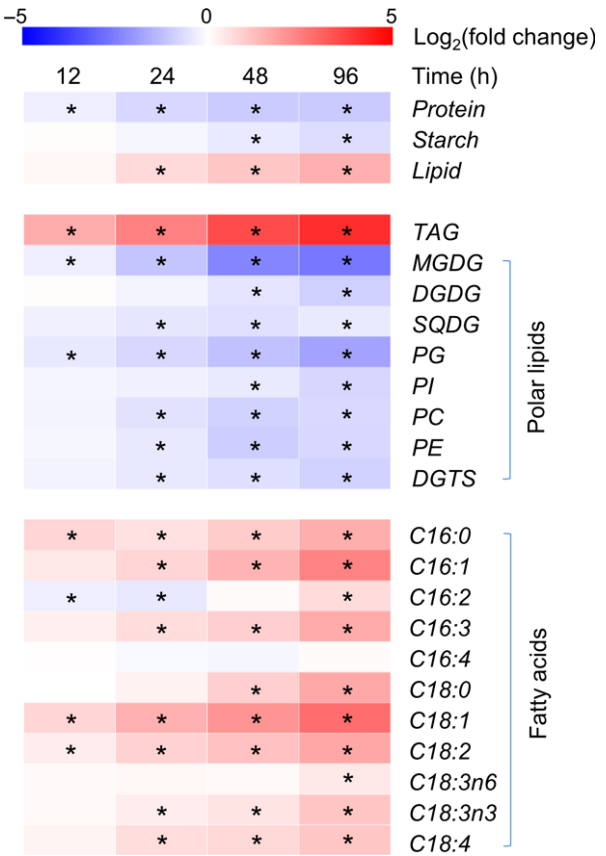

Figure 1. Heat map illustrating the variation of cellular content of major compounds including protein, starch and lipids.
The changes in the compound contents in response to ND were expressed as $\log_2$(fold change) values (relative to 0 h of ND) and displayed in the heat map. Time refers to the duration (in hours) upon ND. Data represent mean ± SD (n = 3). Significant difference (t-test, $P < 0.01$) is indicated with an asterisk.

2017), were aligned with no less than one read (FPKM [fragments per kilobase of transcript per million mapped reads] value ≥ 1) in either biological sample (Data S1). The FPKM values at different time points had a similar range distribution, covering more than six orders of magnitude (Figure S3a). In response to ND, the relative changes ($\log_2$ values, normalized to 0 h) of most transcripts fell between −1 and 1 regardless of the culture time points (gray box in Figure S3b). Among the top 100 genes having most abundant transcripts under favorable growth conditions (0 h of ND), 16% were involved in photosynthesis and 60% were in cellular process translation (Data S2). Upon ND, although most top 100 genes were downregulated considerably, a few maintained a high level of transcripts, e.g., Cz09g11130 (median FPKM = 6968), an unknown gene and Cz05g37140 (median FPKM = 4767), a fructose-bisphosphate aldolase gene. Furthermore, Cz09g30220, an acyl carrier protein gene, was upregulated by ND with a median FPKM value being 7223. The promoter regions of these genes are ideal candidates for driving the constitutive and high expression of transgenes in the future genetic engineering experiments. Interestingly, among the top 100 most upregulated genes, some exhibited an extremely low abundance of basal transcripts and were dramatically induced by ND, e.g., Cz01g09270 (basal FPKM = 0, up to 3600-fold upregulation by ND), an unknown gene and Cz03g37180 (basal FPKM = 0.13, up to 1300-fold upregulation by ND), a putative diamine oxidase gene (Data S2). The promoter regions of these genes are of great interest when expressing transgenes that may cause adverse effects on cell growth under favorable conditions.

According to the definition of differentially expressed gene (DEG) described in Experimental Procedures, 5693 genes were assigned as ND-responsive DEGs (Data S3), which were grouped into 18 clusters based on their temporal expression patterns (Figure 2a). Eight clusters, namely, C1, C5, C6, C10, C11 and C13-C15 were downregulated, while the other 10 clusters were upregulated. According to Li *et al.* (2014), the genes in each cluster were manually categorized into 12 groups (Figure 2b and Data S4) to dissect if a given expression pattern was linked to any specific functions. The genes in the Function unknown category had the greatest percentage in all clusters except C1, ranging from 24 to 57%. C1, predominated by the category Photosynthesis (47%) (Figure 2b and Data S4), was the most severely downregulated cluster, in which gene transcripts dropped sharply upon ND (Figure 2a). For the other 17 clusters, the second largest category was represented by a group of functional genes. For example, the primary functional genes in the clusters C2, C4, C8 and C12 belonged to Metabolism, accounting for 23–32% of the total genes in each corresponding cluster; all four clusters saw the highest induction after 3 h of ND and thereafter maintained a relatively stable upregulation at various levels (Figure 2). By contrast, the category Protein synthesis, modification, folding and turnover was enriched in downregulated clusters including C5, C11 and C13, accounting for 21–29% of the total genes in each corresponding cluster. Similarly, the category DNA, RNA and gene expression was enriched in downregulated clusters (C10, C11, C13 and C14), representing the largest or second largest functional group in each corresponding cluster. The DEGs shared by all ND time points (3–24 h) and specific to early ND (3 h) or late ND (24 h) were also analyzed (Data S5 and Figure S4).

Considering the particular interest of this study in ND-induced lipid metabolism, the related genes were listed in Table S5. Of the 188 lipid metabolism-related genes, 102 were DEGs with 79% and 21% being up and downregulated, respectively; the upregulated DEGs were enriched in C8 and C12. The regulation of lipid metabolism and other pathways upon ND in *C. zofingiensis* are discussed in detail in the subsequent corresponding sections.

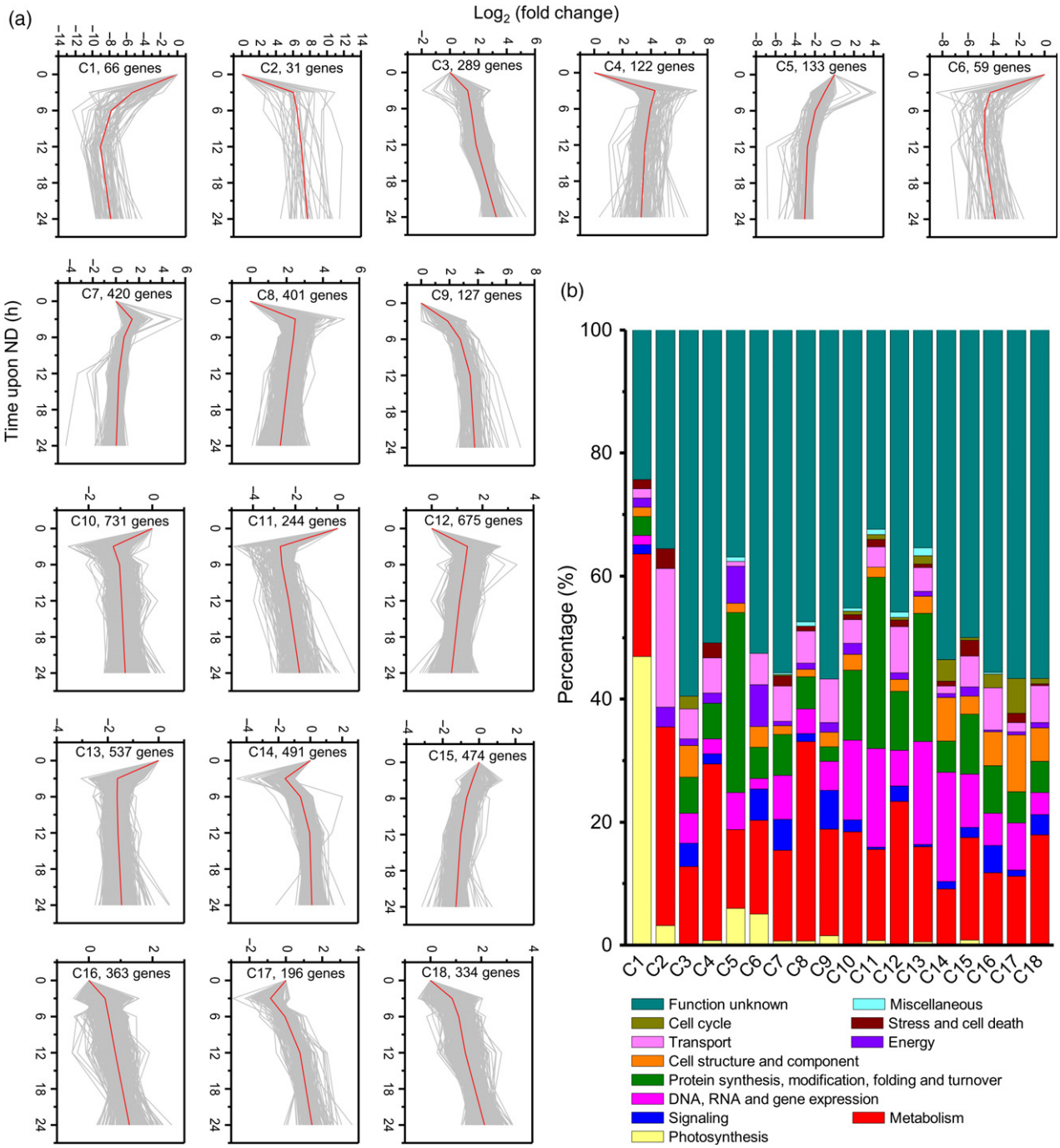

Figure 2. Transcriptional patterns and functional categories of the 5693 DEGs.
(a) Temporal expression patterns of the DEGs grouped into 18 clusters. The values were expressed as $\log_2$(fold change) relative to 0 h of ND and the mean value in each cluster was indicated by a red line.
(b) Functional distribution of DEGs in each cluster.

TAG synthesis involves coordinated stimulation of multiple biological processes

Carbon reallocation to lipids at the expense of protein and starch. ND impaired photosynthesis of *C. zofingiensis* as indicated by the considerable decline in *Fv*/*Fm* and chlorophyll content (Figure S5). Consistently, a severe reduction in transcriptional abundance was observed for genes involved in photosynthesis (Table S6) and the Calvin–Benson cycle (Table S7), indicative of severely attenuated CO_2 fixation. So to support the large demand of

carbon precursors for TAG synthesis, *C. zofingiensis* should reallocate carbon from other sources such as protein and starch, the major biomass components under non-stress conditions (Figure 1 and Table S1).

Upon ND, most of the genes encoding ribosomal proteins, tRNA-synthetases and translation elongation factors were severely downregulated, together with the upregulation of many genes encoding proteolysis-related proteins such as protease and peptidase (Table S8), supporting the net degradation of protein and, therefore, the considerably decreased protein level (Figure 1). Furthermore, the biosynthesis of most amino acids was downregulated in response to ND, accompanied by the upregulated catabolism of many amino acids (Table S9). Accordingly, a drop in the content of free amino acids was observed, including glutamine and glutamate, the most abundant free amino acids in algae (Park *et al.*, 2015) and histidine, lysine, arginine, alanine (Table S2). Interestingly, some free amino acids, such as aromatic amino acids (phenylalanine and tyrosine) and leucine/isoleucine saw an increase upon ND (Table S2), possibly due to the protein degradation that dominated the catabolism of these amino acids. The overall degradation of protein and amino acids probably contributed to replenishment of intermediates in the TCA cycle for recycling the protein-derived carbon and producing energy to meet the enhanced synthesis of fatty acids/TAG. In addition, downregulated biosynthesis and upregulated catabolism of purines and pyrimidines (Table S10), together with a drop in many intermediate metabolites (Table S2) and total RNA (Figure S6), supported the enhanced degradation of purines and pyrimidines from RNA breakdown. The nitrogen salvaged from protein/amino acids and RNA is likely to be repartitioned to those most needed functions for maintaining cell viability against ND stresses and producing storage lipids (Park *et al.*, 2015; Chen *et al.*, 2017).

Starch content remained relatively stable during the first 24 h of ND and then declined gradually (Figure 1), differing from previous reports of green algae such as *Chlamydomonas* and *Chlorella* strains in which starch exhibited a sharp transient increase before decline (Li *et al.*, 2010; Zhu *et al.*, 2014). This may be explained in part by the differential transcriptional regulation: many genes involved in starch synthesis were upregulated in *Chlamydomonas* (Blaby *et al.*, 2013), but just changed minimally in *C. zofingiensis* (Figure 3). The degradation of starch follows two distinct pathways: formation of glucose-6-phosphate (G6P) catalyzed by starch phosphorylase (SPL) and phosphoglucomutase (PGM) and formation of glucose catalyzed by a series of enzymes including starch debranching enzyme (SDBE) and amylase. Both pathways were upregulated by ND (Figure 3 and Table S11). Taken together, starch synthesis remained constant, while starch catabolism was upregulated in response to ND, leading to net starch degradation by which *C. zofingiensis* diverts photosynthetically fixed carbon to fatty acids/TAG via the glycolysis pathway (Figure 3a).

Upregulation of glycolysis and downregulation of gluconeogenesis. The *C. zofingiensis* genome possesses all glycolysis components (Table S11), but neither the chloroplastic nor the cytosolic glycolysis pathway is complete suggested by the subcellular localization prediction (Figure 3 and Data S6). Glucose phosphorylation represents the first irreversible step of glycolysis, catalyzed by hexokinase (HK) or glucokinase (GLK); both are predicted to be

Figure 3. Regulation of central carbon metabolism in response to ND.

(a) Transcriptional regulation of central carbon metabolic pathways. Arrows in red, blue and black indicate transcriptional upregulated, downregulated and non-regulated steps. For proteins encoded by multiple copies of genes, the changes in total transcripts of the isogenes were employed for determining the overall regulation pattern.

(b) Heat map showing $\log_2$(fold change) values of transcripts relative to 0 h of ND. Significant difference (absolute $\log_2$(fold change) value >1 and FDR adjusted $P < 0.01$; $n = 3$) is indicated with an asterisk. Time refers to the duration (in hours) upon ND. The section with the italic Roman numerals right behind the heat map shows the binned transcript abundance at the reference time point (0 h of ND). Five abundance categories are defined: I: below 50% percentile abundance (FPKM < 28), II: 50–75% percentile abundance (28 ≤ FPKM < 62), III: 75–90% percentile abundance (62 ≤ FPKM < 129), IV: 90–99% percentile abundance (129 ≤ FPKM ≤ 1227), V: >99% percentile abundance (FPKM > 1227). The section right after the italic Roman numerals indicates the predicted subcellular localization of proteins (Data S6). Compounds are highlighted with different colors: red, significantly higher; black, not significantly changed; gray not determined; blue, significantly lower under ND conditions as compared to the control (0 h of ND). C, chloroplast; Cy, cytosol; M, mitochondrion; ER, endoplasmic reticulum; O, other. AAC, ATP/ADP carrier; ACH, aconitate hydratase; ACL, ATP-citrate lyase; ACS, acetyl-CoA synthetase; AGPase, ADP-glucose pyrophosphorylase; ALDH, aldehyde dehydrogenase; AMYA, alpha-amylase; AMYB, beta-amylase; BASS, Bile acid-sodium symporter; CIS, citrate synthase; CIT, citrate; DHAP, dihydroxyacetone phosphate; ENO, enolase; FBA, fructose-bisphosphate aldolase; FBP, fructose-1,6-bisphosphatase; FHD, fumarate hydratase; F1,6P, fructose-1,6-biphosphate; F6P, fructose-6-phosphate; FUM, fumarate; GAP, glyceraldehyde 3-phosphate; GAPDHN, glyceraldehyde 3-phosphate dehydrogenase, nonphosphorylating; GAPDH, glyceraldehyde 3-phosphate dehydrogenase; GBSS, granule bound starch synthase; GK, glucokinase; GlcT, plastidic glucose transporter; GLPT, glycerol-3-phosphate transporter; G1P, glucose-1-phosphate; G3P, glycerol-3-phosphate; G6P, glucose-1-phosphate; HK, hexokinase; G6PD, lucose-6-phosphate 1-dehydrogenase; GPDH, glycerol-3-phosphate dehydrogenase; ICT, isocitrate; MAL, malate; MDH, malate dehydrogenase; ME, malic enzyme; MPC, mitochondrial pyruvate carrier; NTT, ATP/ADP antiporter; OAA, oxaloacetate; 2OG, 2-oxoglutarate; OGDH, 2-oxoglutarate dehydrogenase; OPP, oxidative pentose phosphate pathway; PDHC, pyruvate dehydrogenase complex; PEP, phosphoenolpyruvate; PFK, 6-phosphofructokinase; 1,3PGA, 1,3-bisphosphoglycerate; 2PGA,2-phosphoglycerate; 3PGA, 3-phosphoglycerate; PGAM, phosphoglycerate; PK, pyruvate kinase; 6PGD, 6-phosphogluconate dehydrogenase; PGI, glucose-6-phosphate isomerase; PGK, phosphoglycerate kinase; PGLS, 6-phosphogluconolactonase; PGM, phosphoglucomutase; PPT, phosphoenolpyruvate/phosphate translocator; PYC, pyruvate carboxylase; PDC, pyruvate decarboxylase; SBE, starch branching enzyme; SCA, succinyl-CoA; SPL, starch phosphorylase; SPPT, sugar phosphate/phosphate translocator; SCS, succinyl-CoA synthetase; SDBE, starch debranching enzyme; SDH, succinate dehydrogenase; SSS, soluble starch synthase; SUC, succinate; TIM, triosephosphate isomerase; TPT, triose phosphate/phosphate translocator.

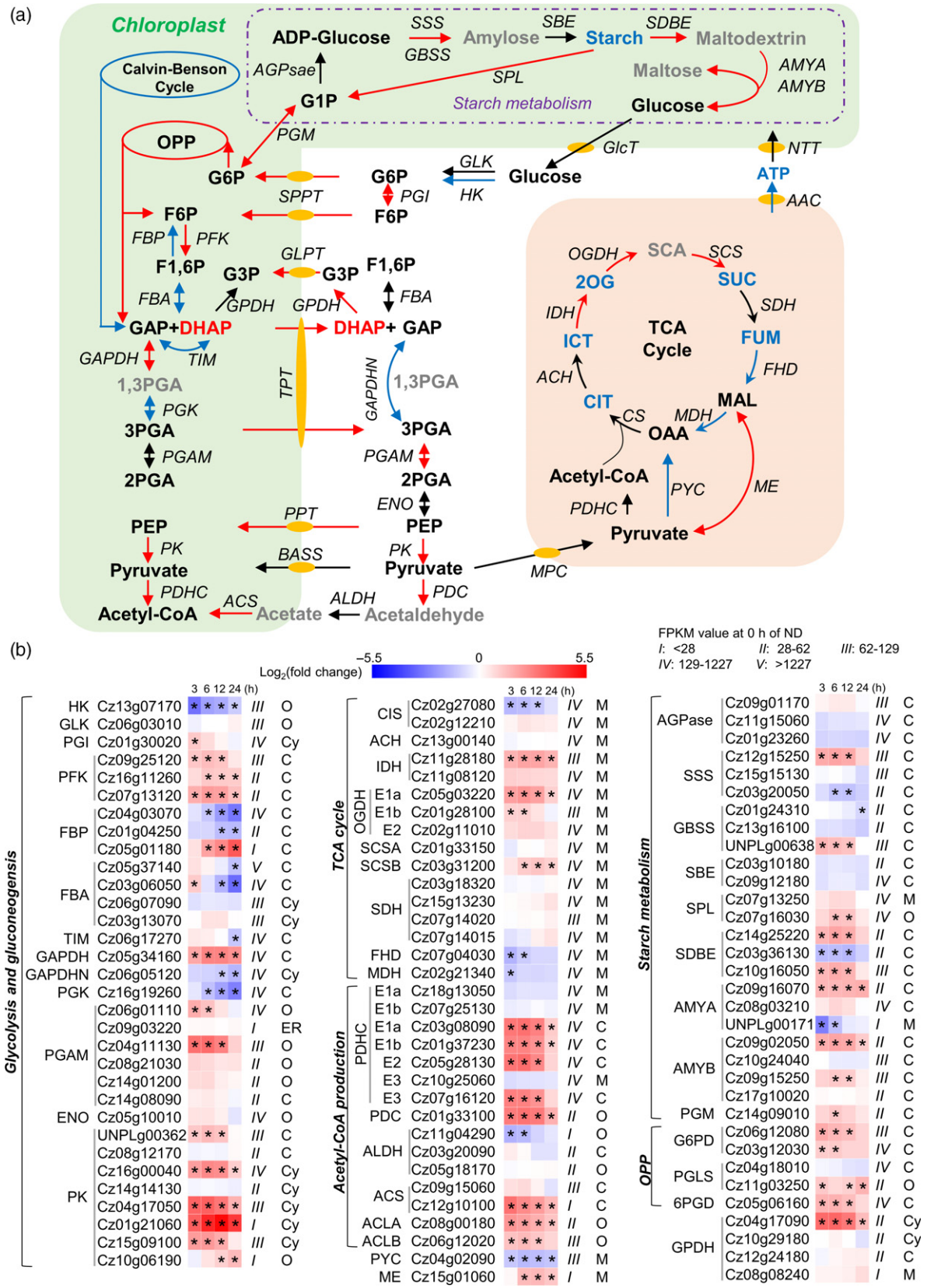

localized in the cytosol (Figure 3). By contrast, phosphofructokinase (PFK), the rate-limiting enzyme responsible for the second irreversible step of glycolysis, has three chloroplastic isoforms. As for pyruvate kinase (PK) catalyzing the last irreversible step of glycolysis, *C. zofingiensis* possesses multiple isoforms of both chloroplast and cytosol. A considerable increase was observed for PFK- and PK-encoding genes (~2- to 40-fold) upon ND (Figure 3), indicative of the strong upregulation of glycolysis. It is worth noting that three upregulated cytosolic *PK* genes (Cz16g00040, Cz04g17050 and Cz15g09100) had higher basal transcript levels than chloroplastic *PK* genes and were more highly upregulated by ND (Table S11). This suggests that cytosolic glycolysis may contribute relatively more to pyruvate generation in *C. zofingiensis*, consistent with the results in *Chlamydomonas* (Klein, 1986). There are some transporters localized in chloroplast envelope to facilitate the exchange of sugar metabolites between the chloroplast and the cytosol (Rawsthorne, 2002; Linka and Weber, 2010). The presence of these transporter genes in *C. zofingiensis* and their upregulation upon ND allowed sugar intermediate translocation for the completion of glycolysis (Figure 3 and Table S12). Gluconeogenesis, an opposite pathway to glycolysis, consists of four irreversible reactions, among which fructose-1,6-bisphosphatase (FBP) is the rate-limiting enzyme. Three FBP-encoding genes were identified in the *C. zofingiensis* genome and responded differentially to ND, yet with overall downregulation (Table S11). Most metabolites in glycolysis/gluconeogenesis were detected and all, except dihydroxyacetone phosphate, showed no significant change in response to ND (Figure 3a and Table S2). Consequently, by enhancing glycolysis and attenuating gluconeogenesis, ND led to more carbon flux to pyruvate, which can be converted to acetyl-CoA for fatty acid synthesis.

Upregulation of multiple acetyl-CoA synthetic pathways. Acetyl-CoA, the precursor for building fatty acids, is derived from multiple routes: from pyruvate mediated by pyruvate dehydrogenase complex (PDHC) or PDHC bypass route, from citrate via ATP-citrate lyase (ACL), from acetylcarnitine by carnitine acetyltransferase, etc. (Rawsthorne, 2002). Genes encoding enzymes involved in the first three routes were identified in *C. zofingiensis*; these were upregulated by ND (Figure 3 and Table S11). It can be noted that PDHC-encoding genes had much higher transcript levels than those involved in the PDHC bypass route (Table S11) and that ACL enzymes catalyzed the production of cytosolic acetyl-CoAs not for fatty acid synthesis in higher plants (Rawsthorne, 2002). Therefore, it appears that in *C. zofingiensis* PDHC and PDHC bypass routes, particularly the former, are used to supply acetyl-CoA in the chloroplast for *de novo* fatty acid synthesis.

Upregulation of fatty acid synthesis and membrane lipid turnover. *De novo* fatty acid synthesis in the chloroplast starts from acetyl-CoA and involves a set of enzymes (Li-Beisson *et al.*, 2015). Searching the *C. zofingiensis* genome identified all genes involved in *de novo* fatty acid synthesis that were considerably upregulated in a well coordinated way (enriched in C8) (Table S5 and Figure S7). This strong stimulation is likely to have selected acetyl-CoA for *de novo* synthesis of fatty acids, therefore preventing acetyl-CoA buildup and promoting accumulation of C16:0, C18:0 and C18:1 (Figure S7). Once incorporated into membrane lipids, the *de novo* synthesized fatty acids can be further desaturated to different levels by a series of desaturases, including omega-6 fatty acid desaturase such as FAD2 (Cz03g33220) and FAD6 (Cz08g04110 and Cz11g21120), omega-3 fatty acid desaturase FAD7 (Cz06g28130 and Cz04g31180), MGDG Δ7 desaturase FAD5 (Cz07g00120, Cz06g00170 and Cz13g01140), MGDG Δ4 desaturase Δ4FAD (Cz06g12050 and UNPLg00012) and Δ3 palmitate desaturase FAD4 (Cz12g10230) (Figure S7). In line with the upregulation of FAD-encoding genes, most unsaturated fatty acids increased considerably upon ND (Figure 1).

Membrane lipid turnover also provided fatty acids for TAG synthesis in *C. zofingiensis*, as indicated by the drastic decrease (42–87%) in membrane lipids (Figure 1) and accumulation of polyunsaturated fatty acids (non-*de novo* synthesized) in TAG (Figure S8), consistent with previous reports of other algae (Li *et al.*, 2012a; Yoon *et al.*, 2012; Liu *et al.*, 2016b; Ma *et al.*, 2016; Wei *et al.*, 2017). Interestingly, no genes involved in the biosynthesis of membrane glycerolipids were downregulated by ND. Instead, five of these, particularly DGDG synthase (DGD) were upregulated (Figure S9 and Table S5). We hypothesized that, under ND conditions, the expression level of these genes remained, contributing to the continuing synthesis of membrane glycerolipids. Lipases responsible for membrane lipid degradation, conversely, are greatly upregulated leading to net decrease in these lipids. Some putative membrane lipase-encoding genes were found to be upregulated by ND in *Chlamydomonas* (Miller *et al.*, 2010; Goodenough *et al.*, 2014). Among these, PGD1 has proven to be involved in MGDG turnover for TAG synthesis (Li *et al.*, 2012a). In *C. zofingiensis*, Cz01g38020, a homologue of *Chlamydomonas* PGD1, was drastically upregulated (~15-fold) by ND (Figure 4a and Table S5). This is coincident with severe MGDG degradation (Figure 1), indicating the similar role of PGD1 in *C. zofingiensis*. However, PGD1 acts only on *de novo* synthesized MGDG [mainly 18:1n9/16:0 (sn-1/sn-2)] releasing C18:1n9 as the main product (Li *et al.*, 2012a). Furthermore, other membrane lipids also decreased (Figure 1), indicating the involvement of additional lipases. In total, 18 lipase genes were upregulated over two-fold in *C. zofingiensis* (Figure 4a). Cz02g15090 and Cz03g14190, clustering with PGD1 (Cz01g38020),

represent two of the most highly upregulated genes and may work synergistically with Cz01g38020 to recycle membrane lipids especially galactolipids. In addition, three of five upregulated patatin-like phospholipase genes (UNPLg00084, UNPLg00117 and Cz01g30230) exhibited an upregulation expression pattern, indicating their involvement in recycling fatty acids from phospholipids for TAG synthesis. Cz02g13210, a putative monoglyceride lipase gene with the most highest fold change level of upregulation (~40-fold), may work with Cz02g36160, a putative DAG lipase, to recycle membrane lipid-derived DAG for TAG assembly.

Enhanced provision of energy and reductant. Fatty acid synthesis requires substantial amounts of ATP (energy) and NADPH (reductant). Considering the severely inhibited photosynthesis by ND, enhancement of other sources of ATP and NADPH is required. To support the enhanced synthesis of fatty acids (Figure 1), *C. zofingiensis* consumed increased amounts of ATP leading to a severe decrease in ATP levels and an increase in the ratios of ADP/ATP and AMP/ATP (Table S2). Therefore, ATP production should be boosted to meet energy needs, this is indicated by several lines of evidence: (i) upregulation of glycolysis producing more ATP via substrate level phosphorylation (Figure 3 and Table S11); and (ii) upregulation of isocitrate dehydrogenase (IDH), 2-oxoglutarate dehydrogenase (OGDH) and succinyl-CoA synthetase (SCSA) genes in the TCA cycle: the IDH enzyme produces ATP while OGDH and SCSA produce NADH molecules that enter oxidative phosphorylation for ATP production in the mitochondria (Figure 3 and Table S12). A decrease was observed for the intermediates of the TCA cycle such as citrate, isocitrate, 2-oxoglutarate and succinate (Figure 3a and Table S2), in agreement with the results in *C. reinhardtii* (Park *et al.*, 2015). The amino acids from protein degradation may replenish the TCA cycle to support its upregulation.

Multiple pathways contribute to the production of NADPH (Ratledge, 2014). One is the oxidative pentose phosphate (OPP) pathway, in which glucose-6-phosphate dehydrogenase (G6PDH) and 6-phosphogluconate dehydrogenase (6PGD) catalyze the two NADPH-producing steps. *C. zofingiensis* has two G6PDH-encoding genes (Cz06g12080 and Cz03g12030) and one 6PGD-encoding gene (Cz05g06160), all predicted to be chloroplast-localized (Data S6) and upregulated in a similar expression pattern within cluster C12 (Table S12). $NADP^+$-dependent malic enzyme (ME) also plays an important role in the provision of NADPH via converting malate to pyruvate. In *C. zofingiensis*, five $NADP^+$-dependent ME-encoding genes were annotated (Table S7), with one predicted to be in the chloroplast (Cz15g18140) and four probably in the cytosol (Cz07g26110, Cz04g02110, Cz09g11240 and Cz06g32210) (Data S6). Upon ND, the four cytosolic *ME* genes responded differently at the mRNA level but their overall abundance was only slightly changed; by contrast, the chloroplastic gene level was considerably upregulated ~4.7-fold, following a similar expression pattern (within cluster C8) as genes involved in the NADPH-requiring steps of *de novo* fatty acid synthesis including *KAR* (Cz01g34370), *ENR* (Cz11g20040) and *SAD* (Cz04g09090). Other $NADP^+$-dependent enzymes may also contribute to NADPH generation, including glyceraldehyde 3-phosphate dehydrogenase (GAPHD; Cz06g05120), malate dehydrogenase (MDH; Cz01g16230 and Cz04g33150) and isocitrate dehydrogenase (IDH; Cz12g16160). These genes, however, were all downregulated to different extents by ND (Data S1). Therefore, it is likely G6PDH, 6PGD and ME in *C. zofingiensis* support the increasing demand for NADPH to synthesize fatty acids under ND conditions.

Upregulation of TAG assembly pathways. TAG assembly in the acyl-CoA-dependent pathway requires the input of substrates, glycerol-3-phosphate (G3P) and acyl-CoA (Ohlrogge and Browse, 1995). G3P can be derived from dihydroxyacetone phosphate catalyzed by G3P dehydrogenase (GPDH) or from glycerol catalyzed by glycerol kinase (GK), while acyl-CoAs come from fatty acids (*de novo* synthesized and/or membrane-recycled) mediated by long-chain acyl-CoA synthetase (LACS). Overall, *GPDH*, *GK* and *LACS* genes were upregulated by ND to support elevated TAG assembly (Tables S5 and S11).

G3P acyltransferase (GPAT) catalyzes the first committed step of acyl-CoA-dependent TAG assembly. Unlike higher plants that generally contain a high dose of GPAT isoforms, e.g. nine for Arabidopsis (Körbes *et al.*, 2016), *C. zofingiensis* possessesed only two putative GPAT-encoding genes (Figure 4b). Cz11g03260 (GPAT1), predicted to be chloroplast-targeted, was downregulated moderately (~2.3-fold). By contrast, Cz09g31330 (GPAT2), a homologue of Arabidopsis ER-targeted GPAT9, was considerably upregulated by ND (>4-fold) (Figure 4b and Table S5). Lysophosphatidic acid acyltransferase (LPAAT) mediates the second acylation leading to the formation of phosphatidic acid (PA). *C. zofingiensis* contains three putative LPAAT isoforms: Cz16g02090, a homologue of *C. reinhardtii* chloroplastic LPAAT (LPAAT1) (Yamaoka *et al.*, 2016), Cz04g14150, a homologue of *C. reinhardtii* ER LPAAT (LPAAT2) (Kim *et al.*, 2018) and Cz10g20070. The former two were greatly upregulated (~3.9- and 4.7-fold, respectively), whereas the third gene showed just a slight upregulation (<2-fold) upon ND (Figure 4b and Table S5). Diacylglycerol (DAG), the acyl acceptor for the last-step TAG assembly, is mainly from PA mediated by phosphatidate phosphatase (PAP). *C. zofingiensis* genome encodes three putative PAP isoforms: the chloroplastic *PAP* (Cz05g23060) was upregulated considerably (~4.5-fold) upon ND, by contrast the extrachloroplastic isoforms

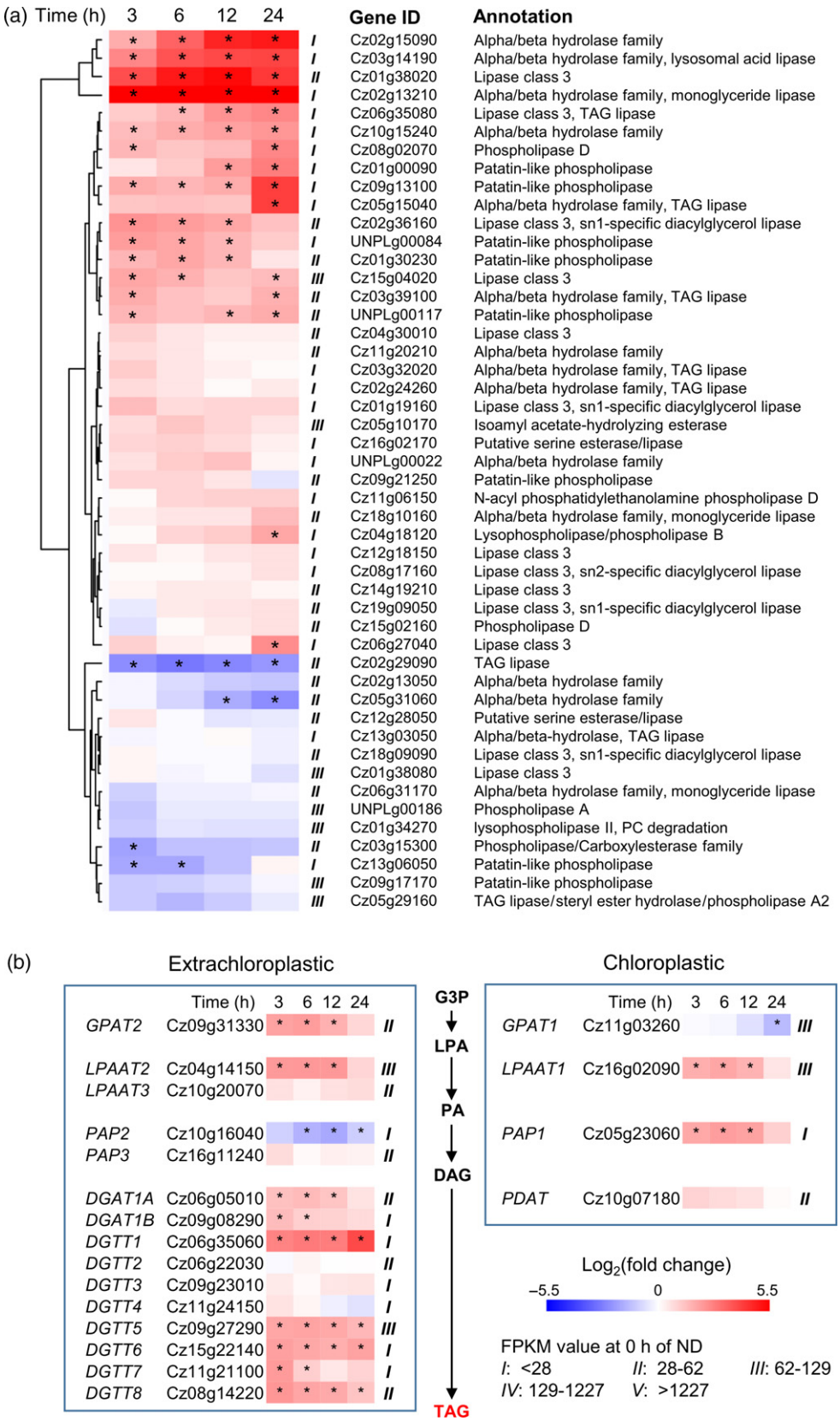

Figure 4. Regulation of lipases (a) and TAG assembly (b) in response to ND.
Heat map shows $\log_2$(fold change) values of transcripts relative to 0 h of ND. Significant difference (absolute $\log_2$(fold change) value >1 and FDR adjusted $P < 0.01$; $n = 3$) is indicated with an asterisk. Time refers to the duration (in hours) upon ND. The section with the italic Roman numerals right behind the heat map shows the binned transcript abundance at the reference time point (0 h of ND). See Figure 3 for the definition of abundance categories. The subcellular localization prediction see Data S6. DAG, diacylglycerol; DGAT, Diacylglycerol *O*-acyltransferase; DGAT1, type I DGAT; DGTT, type II DGAT; G3P, glycerol-3-phosphate; GPAT, glycerol-3-phosphate acyltransferase; LPA, lysophosphatidic acid; LPAAT, 1-acyl-sn-glycerol-3-phosphate acyltransferase; PAP, phosphatidate phosphatase; PDAT, phospholipid:diacylglycerol acyltransferase; TAG, triacylglycerol.

Cz10g16040 and Cz16g11240 were downregulated (Figure 4b and Table S5). These results suggested an important role of the extrachloroplastic GPAT, both chloroplastic and extrachloroplastic LPAATs and the chloroplastic PAP in ND-induced TAG accumulation.

The last step of TAG synthesis is catalyzed by either DAG acyltransferase (DGAT) or phospholipid:diacylglycerol acyltransferase (PDAT). According to Roth *et al.* (2017), 11 putative DGAT-encoding genes from *C. zofingiensis* were annotated, but two of these have exact the same coding sequence. With the assistance of our RNA-seq data, we updated their coding sequences and renamed these based on phylogenetic analysis (Figure S10 and Table S13): two type I DGATs (DGAT1) and eight type II DGATs (DGTT). This number is to date the most DGATs reported for green microalgae. Upon ND, *DGTT2-4* transcripts showed little variation, suggesting their potential roles for non-stress-induced TAG accumulation. The other seven *DGAT* genes were upregulated in differential expression patterns (Figure 4b and Table S5), indicating their distinctive, yet collaborative, roles in modulating TAG composition and levels as stated in *Chlamydomonas* (Liu *et al.*, 2016b) and *Nannochloropsis* (Xin *et al.*, 2017). Unlike DGAT, PDAT transfers an acyl moiety from phospholipids to DAG for TAG synthesis. *C. zofingiensis PDAT* was upregulated by ND, but less than two-fold, suggesting its minor role in ND-induced TAG accumulation as stated in *Chlamydomonas* (Yoon *et al.*, 2012). These TAG assembly-related enzymes, differing in spatial distribution and temporal expression pattern, may work in concert and contribute to the large TAG increase in *C. zofingiensis* (Figure 1). Nevertheless, their interaction and roles in TAG synthesis need to be experimentally demonstrated. In addition, the large upregulation (~8.3-fold) of Cz04g29220, encoding a major lipid droplet protein (MLDP) of green algal lineage that stabilizes lipid droplets (LDs) for TAG storage (Moellering and Benning, 2010), supports the drastic accumulation of TAG for storage in LDs.

The extrachloroplastic GPAT rather than the chloroplastic one contributes to TAG accumulation

To elucidate the role of GPATs in *C. zofingiensis*, both genes were characterized via RNAi-mediated knockdown and overexpression approaches. The gene expression at the transcriptional level was verified by qPCR and two transgenic lines for each knockdown or overexpression were selected. The knockdown efficiency reached ~85% for both *GPAT1* and *GPAT2*, while overexpression led to ~14- and 26-fold increase for *GPAT1* and *GPAT2* transcripts, respectively (Figure 5). Both knockdown and

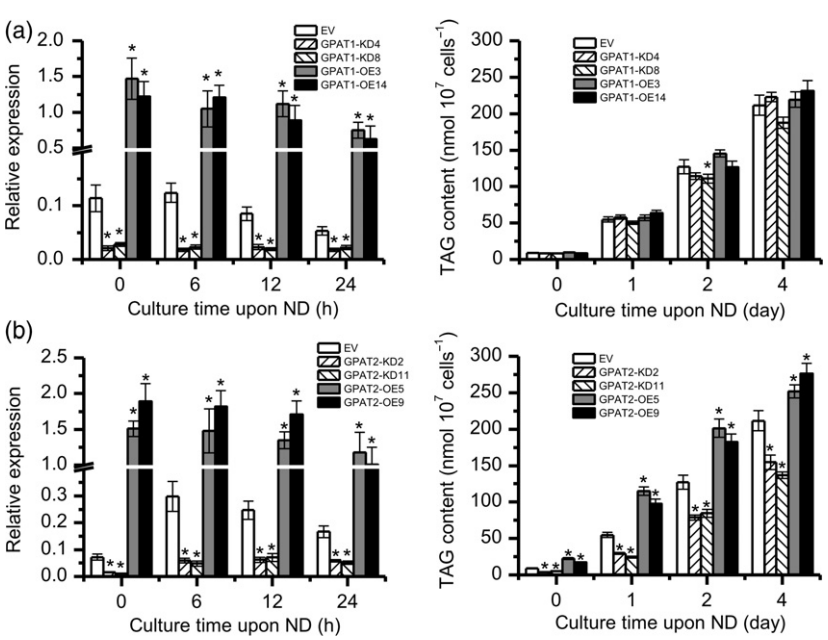

Figure 5. Functional roles of GPAT1 and GPAT2 in TAG accumulation in *C. zofingiensis*.
(a) *GPAT1* transcriptional level and TAG content in the knockdown and overexpression lines of *GPAT1*; (b) *GPAT2* transcriptional level and TAG content in the knockdown and overexpression lines of GPAT2. The transcriptional levels of *GPAT1* and *GPAT2* were expressed as relative values normalized to the internal control β-actin, determined by qPCR. Data represent mean ± SD ($n = 3$). Significant difference (*t*-test, $P < 0.01$) is indicated with an asterisk as compared to the EV control.

overexpression of *GPAT1* had little effect on TAG synthesis (Figure 5a). By contrast, knockdown and overexpression of *GPAT2* resulted in a considerable decrease (~2.2-fold) and increase (2.5-fold) in TAG content, respectively (Figure 5b). These results together confirmed that the extrachloroplastic (ER) *GPAT* rather than the chloroplastic one plays a central role in TAG synthesis and accumulation. This is a pioneering work on the functional characterization of GPAT in green algae and demonstrates the feasibility of using *GPAT* as an engineering target for improving TAG content.

Metabolic regulation of TAG synthesis in *C. zofingiensis*: insights from comparative analysis with other algae

For comparison, three other algae were employed including the model alga *C. reinhardtii* (Blaby *et al.*, 2013), the oleaginous green alga *Monoraphidium neglectum* (Jaeger *et al.*, 2017) and the oleaginous heterokont *N. oceanica* (Li *et al.*, 2014), which all had ND-induced time-resolved transcriptomes. The three green algae differed greatly from *N. oceanica* except for energy production, which was produced mainly by upregulating glycolysis and the TCA cycle (Table 1). There are several key distinctions between *C. zofingiensis* and other two green algae. First, *C. zofingiensis* could utilize mainly the chloroplastic PDHC route to produce acetyl-CoA from pyruvate (Table S11), while *C. reinhardtii* and *M. neglectum* employ the PDHC bypass route as the major way for supplying acetyl-CoA under ND conditions. Second, most genes involved in *de novo* fatty acid synthesis were considerably upregulated in a well coordinated manner by ND in *C. zofingiensis*, while most genes were downregulated to various extents in *C. reinhardtii* as well as in *M. neglectum*. Third, *C. zofingiensis* uses the ER GPAT, instead of the chloroplastic, route for

Table 1 Comparison of the upregulated genes involved in lipid metabolism between *C. zofingiensis* and other algae

Pathways	*C. zofingiensis*	*C. reinhardtii*	*M. neglectum*	*N. oceanica*
Fatty acid synthesis and activation	ACCase (α-CT, β-CT, BC, BCCP), ACCase (cyto), ACP, MCT, KAR, HAD, ENR, KAS I, KAS II, KAS III, FAT, LCAS	ACCase (α-CT), FAT, LCAS	ACCase (α-CT, β-CT, BC), HAD, KAS II, FAT, LCAS	KAS I, FAT
Fatty acid desaturation	SAD, FAD2, FAD4, FAD5, FAD6, FAD7, Δ4/Δ6FAD	SAD, FAD2, FAD5, FAD7, Δ4/Δ6FAD	SAD, FAD2, FAD5, FAD7	SAD, FAD5
Membrane lipid synthesis	DGD, CCT	DGD, SQD2, ETK, EPT, BTA	DGD, CCT	BTA
TAG assembly	GK, GPDH, GPAT (ER), LPAAT (C, ER), PAP (C), DGAT, DGTT	GPDH, GPAT (C), PAP (C), DGAT, DGTT, PDAT	GPDH, LPAAT (C, ER), PAP (C), DGTT	LPAAT (C, ER), PAP (ER), DGAT, DGTT
Acetyl-CoA production	PDHC (E1, E2, E3; C), PDC, ACS, ACL, AK	PDHC (E1, E2; M), PDC, ACL	PDHC (E1; C), PDHC (E1, E2; M), PDC, ALDH, ACS	PDHC (E2, E3; M), PDC, ACS
NADPH production	G6PD, 6PGD, ME (NADP)	G6PD, 6PGD, MDH (NADP)	G6PD, 6PGD, ME (NADP)	ME (NADP)
Energy production	PK (ATP), GAPDH (NADH), SCS (ATP), IDH (NADH), OGDH (NADH), ME (NADH)	PK (ATP), GAPDH (NADH), SCS (ATP), IDH (NADH), MDH (NADH)	PK (ATP), SCS (ATP), IDH (NADH), OGDH (NADH), SDH (NADH), MDH (NADH), ME (NADH)	PK (ATP), SCS (ATP), IDH (NADH), OGDH (NADH), SDH (NADH), ME (NADH)

Gene expression data for *C. reinhardtii*, *M. neglectum* and *N. oceanica* were retrieved from Blaby *et al.* (2013), Jaeger *et al.* (2017) and Li *et al.* (2014), respectively. Cutoff for upregulation: fold change >2. Subcellular localization information: cyto, cytosol; C, chloroplast; ER, endoplasmic reticulum; M, mitochondria. ACCase, acetyl-CoA carboxylase; ACP, acyl carrier protein; ACS, acetyl-CoA synthetase; AK, acetate kinase; ALDH, aldehyde dehydrogenase; ATL, ATP-citrate lyase; BC, biotin carboxylase; BCCP, biotin carboxyl carrier protein; BTA, betaine lipid synthase; CCT, choline-phosphate cytidylyltransferase; CT, carboxyltransferase; DGAT, Diacylglycerol *O*-acyltransferase, type I; DGD, digalactosyldiacylglycerol synthase; DGTT, Diacylglycerol *O*-acyltransferase, type II; ENR, enoyl-ACP reductase; EPT, ethanolaminephosphotransferase; ETK, ethanolamine kinase; FAD, fatty acid desaturase; FAT, acyl-ACP thioesterase; GK, glycerol kinase; GAPDH, glyceraldehyde 3-phosphate dehydrogenase; GPAT, glycerol-3-phosphate acyltransferase; G6PD, glucose-6-phosphate 1-dehydrogenase; 6PGD, 6-phosphogluconate dehydrogenase; GPDH, glycerol-3-phosphate dehydrogenase; HAD, 3-ketoacyl-ACP dehydratase; IDH, isocitrate dehydrogenase; KAR, 3-ketoacyl-ACP reductase; KAS, 3-ketoacyl-ACP synthase; LCAS, long-chain acyl-CoA synthetase; LPAAT, 1-acyl-sn-glycerol-3-phosphate acyltransferase; MCT, malonyl-CoA:acyl carrier protein transacylase; ME, malic enzyme; MDH, malate dehydrogenase; OGDH, 2-oxoglutarate dehydrogenase; PAP, phosphatidate phosphatase; PDAT, phospholipid:diacylglycerol acyltransferase; PDC, Pyruvate decarboxylase; PDHC, pyruvate dehydrogenase complex; PK, pyruvate kinase; SAD, stearoyl-ACP desaturase; SCS, succinyl-CoA synthetase; SDH, succinate dehydrogenase; SQD2, Sulfoquinovosyldiacylglycerol synthase.

ND-induced TAG assembly (Figure 5); by contrast, *C. reinhardtii* is likely to prefer chloroplastic GPAT, which was upregulated by ND (Blaby *et al.*, 2013) for TAG synthesis. Fourth, *C. zofingiensis* contains 10 DGAT genes, while *C. reinhardtii* possesses only six (Miller *et al.*, 2010). The absolute level of DGAT transcripts in *C. zofingiensis* was considerably higher than that in *C. reinhardtii* under both NR (FPKM value: 262 VS 35) and ND (FPKM value: ~835 versus ~145) conditions (Table S5 and Blaby *et al.*, 2013). This may partially explain why *C. zofingiensis* is capable of synthesizing considerably larger amounts of TAG than *C. reinhardtii* under both NR and ND conditions. *C. zofingiensis* also had a considerable higher level of DGAT transcripts than *M. neglectum*, although they had a comparable number of DGAT genes (Jaeger *et al.*, 2017). Fifth, unique to *C. zofingiensis*, TAG and astaxanthin ester, which share common precursors, accumulate in a well coordinated way (Liu *et al.*, 2016a). Sixth, unlike *C. reinhardtii*, which shows a transient increase in starch before degradation, *C. zofingiensis* maintains starch levels followed by a decrease in levels (Figure 1).

Genomewide identification of engineering targets for rational improvement in TAG

Our multiomics study provides insights into identifying potential gene targets for engineering purposes, which are summarized in Table 2. TAG enhancement can be achieved by engineering strategies such as 'pulling' (pulls fatty acids to the glycerol backbone especially DAG), 'pushing' (pushes carbon flux to precursors for fatty acid and TAG syntheses, e.g. acetyl-CoA and G3P) and/or 'protection' (prevents TAG degradation). As the key enzyme catalyzing the committed step of TAG assembly in the Kennedy pathway, DGAT is of great importance and serves as a successful engineering target for TAG improvement by providing pulling force via overexpression, which has been demonstrated in several algae including *C. reinhardtii* (Iwai *et al.*, 2014), *N. oceanica* (Wei *et al.*, 2017; Xin *et al.*, 2017; Zienkiewicz *et al.*, 2017; Mao *et al.*, 2019) and *P. tricornutum* (Dinamarca *et al.*, 2017). Moreover, algal DGATs showed distinctive substrate preferences on acyl-CoAs and their manipulation altered the fatty acid composition of TAG (Liu *et al.*, 2016b; Wei *et al.*, 2017; Xin *et al.*, 2017). In *C. zofinginesis*, of the 10 DGAT genes, *DGAT1A*, *DGTT5* and *DGTT8* showed relatively higher abundances of basal transcripts and were boosted considerably by ND, which correlated well with TAG accumulation (Figure 1and Table S5); these DGAT genes may be potential engineering targets for modulating the content and fatty acid composition of TAG in *C. zofingiensis*. Other acyltransferases involved in TAG assembly such as GPAT and LPAAT are of interest, as they pull fatty acids to glycerol backbones for subsequent TAG synthesis (Iskandarov *et al.*, 2016; Niu *et al.*, 2016; Yamaoka *et al.*, 2016; Balamurugan *et al.*, 2017).

Generating more acetyl-CoA represents a feasible 'pushing' strategy to promote fatty acid synthesis and the subsequent TAG assembly (Yan *et al.*, 2013; Avidan *et al.*, 2015; Rengel *et al.*, 2018). In *C. zofingiensis*, the major sources of acetyl-CoA are catalyzed by chloroplastic PDHC and acetyl-CoA synthetase (ACS), which have the potential to be engineered for promoting fatty acid synthesis. Fatty acid synthesis requires the input of reductants (NADPH). Overexpression of G6PD, 6PGD, or ME genes has been demonstrated in algae, and led to the generation of more NADPH and synthesis of greater amounts of TAG (Xue *et al.*, 2015, 2017; Zhao *et al.*, 2015). This strategy should also be applicable to *C. zofingiensis*. The fatty acids pulled by acyltransferases in the Kennedy pathway are in the form of acyl-CoAs, which can be derived either from acyl-ACPs by the action of FAT and LCAS, or from membrane lipids mediated by lipases and LCAS. Upon ND in *C. zofingiensis*, the single FAT (Cz04g05080), several putative membrane lipid lipases (Cz01g38020, Cz02g15090, Cz03g14190, etc.) and one LCAS (Cz11g20120) were upregulated substantially (Table S5), which are potential targets to enhance the production of acyl-CoAs ready for TAG assembly. In addition to acyl-CoAs, G3P is the other precursor providing the glycerol backbone for TAG assembly, which is derived mainly from DHAP catalyzed by GPDH (Yao *et al.*, 2014; Driver *et al.*, 2017). One of the four GPDH genes in *C. zofingiensis*, Cz04g17090, was considerably upregulated by ND and correlated well with TAG accumulation (Table S11), therefore representing a promising engineering target.

Another option is to protect TAG from being degraded by lipases. There have been several reported algal lipases involved in TAG hydrolysis, e.g. CrLIP1, a DAG-like lipase from *C. reinhardtii* (Li *et al.*, 2012b) and a multifunctional lipase/phospholipase/acyltransferase from *Thalassiosira pseudonana* (Trentacoste *et al.*, 2013). Knockdown of the lipase in the latter report resulted in a considerable increase in TAG (~4-fold) without compromising growth under both nutrient replete and depleted conditions, indicative of the great potential of this strategy for increasing TAG. Several lipases from *C. zofingiensis*, such as Cz02g29090 and Cz05g31060, were downregulated by ND, inversely related to TAG accumulation (Figure 1 and Table S5); they are possibly involved in TAG degradation and represent candidate lipases worthy of engineering. The fatty acids released from TAG are subject to beta-oxidation, which is likely to occur in peroxisomes in algae (Kong *et al.*, 2018). An insertional mutation of acyl-CoA oxidase 2 (ACX2) in *C. reinhardtii* led to 20% increased TAG levels under ND conditions and maintained much higher TAG levels when exposed to N replenishment (Kong *et al.*, 2017), pointing to the feasibility of improving algal TAG through suppressing the fatty acid beta-oxidation pathway. Cz07g30210, a homologue to ACX2 predicted

Table 2 List of potential engineering targets for enhancing TAG synthesis in *C. zofingiensis*

Gene name	Gene ID	Putative function	Expression pattern upon ND	Strategy
Pulling				
DGAT, DGTT	Cz06g05010, Cz09g08290, or Cz08g14220	Transfers the acyl moiety from acyl-CoAs to DAG for TAG synthesis	Upregulated within cluster C12 (Cz06g05010) or C8 (Cz09g08290 and Cz08g14220)	Overexpression
GPAT	Cz09g31330	Transfers the acyl moiety from acyl-CoAs to G3P for LPA synthesis	Upregulated within cluster C8	Overexpression
LPAAT	Cz16g02090	Transfers the acyl moiety from acyl-CoAs to LPA for PA synthesis	Upregulated within cluster C12	Overexpression
Pushing				
PDHC	Cz03g08090 or Cz01g37230	Produces acetyl-CoA from pyruvate	Upregulated within cluster C8	Overexpression
ACS	Cz12g10100	Produces acetyl-CoA from acetate	Upregulated within cluster C8	Overexpression
G6PD	Cz06g12080 or Cz03g12030	Provides NADPH	Upregulated within cluster C12	Overexpression
6PGD	Cz05g06160	Provides NADPH	Upregulated within cluster C12	Overexpression
ME	Cz15g18140	Produces pyruvate and NADPH from malate	Upregulated within cluster C8	Overexpression
FAT	Cz04g05080	Releases fatty acids off acyl-ACPs	Upregulated within cluster C8	Overexpression
Membrane lipid lipases	Cz01g38020, Cz02g15090, or Cz03g14190	Releases fatty acids off membrane lipids	Upregulated within cluster C9	Overexpression
LACS	Cz11g20120	Synthesizes acyl-CoAs from free fatty acids	Upregulated within cluster C8 (Cz11g20120)	Overexpression
GPDH	Cz04g17090	Converts DHAP to G3P	Upregulated within cluster C8	Overexpression
Protection				
MLDP	Cz04g29220	Stabilizes LDs for TAG storage	Upregulated within cluster C8	Overexpression
Lipases for TAG, DAG and MAG	Cz02g29090 or Cz05g31060	Hydrolysis of TAG, DAG and MAG	Downregulated within cluster C13 (Cz02g29090) or C15 (Cz05g31060)	Knockdown or knockout
AOX	Cz07g30210	Fatty acid degradation	Little change up ND	Knockdown or knockout
LACS, peroxisomal	Cz12g27140	Synthesizes acyl-CoAs from free fatty acids	Little change up ND	Knockdown or knockout
Transcription factors				
MYB	Cz10g24240 or Cz06g23090	MYB family transcription factor with global control of TAG	Upregulated within cluster C12 (Cz06g23090) or C8 (Cz10g24240)	Overexpression
bHLH	Cz03g20070 or UNPLg00160	bHLH family transcription factor with global control of TAG	Upregulated within cluster C12 (Cz03g20070) or C8 (UNPLg00160)	Overexpression
bZIP	Cz15g21170 or UNPLg00449	bZIP family transcription factor with global control of TAG	Upregulated within cluster C12 (Cz15g21170) or C8 (UNPLg00449)	Overexpression

ACS, acetyl-CoA synthetase; AOX, acyl-CoA oxidase; DGAT, diacylglycerol *O*-acyltransferase, type I; DGTT, diacylglycerol *O*-acyltransferase, type II; FAT, acyl-ACP thioesterase; GPAT, glycerol-3-phosphate acyltransferase; G6PD, glucose-6-phosphate 1-dehydrogenase; 6PGD, 6-phosphogluconate dehydrogenase; GPDH, glycerol-3-phosphate dehydrogenase; LACS, long-chain acyl-CoA synthetase; LPAAT, 1-acyl-sn-glycerol-3-phosphate acyltransferase; MLDP, major lipid droplet protein; ME, malic enzyme; PDHC, pyruvate dehydrogenase complex.

in the peroxisome, may be manipulated via knockdown/knockout to protect fatty acids from oxidation and, therefore, promote TAG levels in *C. zofingiensis*. Before beta-oxidation initiated by ACX, fatty acids need to be activated to form acyl-CoAs, this is catalyzed by a peroxisomal LACS (different from the above-mentioned LACSs involved in TAG synthesis). Suppression of this gene, which has not been proposed before, could be able to inhibit the fatty acid beta-oxidation pathway and, therefore, result in TAG elevation. Cz05g30060, a predicted peroxisomal LACS, is such a target for engineering in *C. zofingiensis*.

TAG synthesis and accumulation involves a series of collaborative steps and manipulation of a single gene, mentioned above, generally cannot achieve a satisfactory increase. Transcription factors (TFs) involved in TAG metabolism are of particular interest because they control a set of genes for TAG synthesis. Using these genes as the engineering target could bypass the manipulation of multiple genes and achieve better performance in promoting TAG production (Gargouri *et al.*, 2015; López García de Lomana *et al.*, 2015). Moreover, TAG induction generally involves abiotic stress conditions, leading to ultimate growth

reduction. The manipulation of TF has the potential to turn on TAG accumulation under non-stress conditions, thereby avoiding the use of stress conditions and compromised growth, and having great benefit for biotechnological applications. It has been demonstrated that overexpression of certain TFs in algae has led to enhanced lipid synthesis to various extents (Zhang *et al.*, 2014; Kang *et al.*, 2015, 2017; Kwon *et al.*, 2018). In *C. zofingiensis*, several TFs from the MYB family (e.g., Cz10g24240), bHLH family (e.g. Cz03g20070) and bZIP family (e.g. Cz15g21170), which are predicted to regulate lipid metabolism for TAG accumulation based on co-expression analysis (Table S14 and Data S7), represent the most interesting targets of engineering for maximized output of TAG.

CONCLUSIONS

Taken together, our results have laid out a solid basis to better understand TAG synthesis in *C. zofingiensis* (Figure 6). Rapid TAG accumulation induced by ND involved the coordinated upregulation of 'pushing', 'pulling' and 'protection' including: (i) carbon reallocation from protein and starch; (ii) PDHC and PDHC bypass pathways for producing acetyl-CoAs; (iii) *de novo* fatty acid synthesis, fatty acid desaturation and membrane lipid turnover for acyl-CoAs; (iv) G3P production; (v) acyltransferase for TAG assembly and MLDP for TAG packaging into LDs; (vi) glycolysis and TCA cycle for energy; and (vii) OPP pathway and chloroplastic NADP-ME for NADPH. It is worth noting that the significant change in expression of a gene at the transcriptional level does not necessarily mean it has a critical function and requires additional layers of evidence for confirmation. In this context, we chose GPAT, the first acyltransferase for TAG assembly in the Kennedy pathway, for functional characterization and demonstrated that extrachloroplastic GPAT, rather than chloroplastic GPAT, played an important role in ND-induced TAG accumulation, in agreement with the RNA-seq data. Furthermore, genome-wide analysis identified several potential TFs that regulate global lipid metabolism. Identification of the key functional genes and understanding the regulatory mechanisms involved in TAG biosynthesis, together with the annotated genome sequence and established transformation system, should pave the way for trait improvement via rational genetic engineering in this alga.

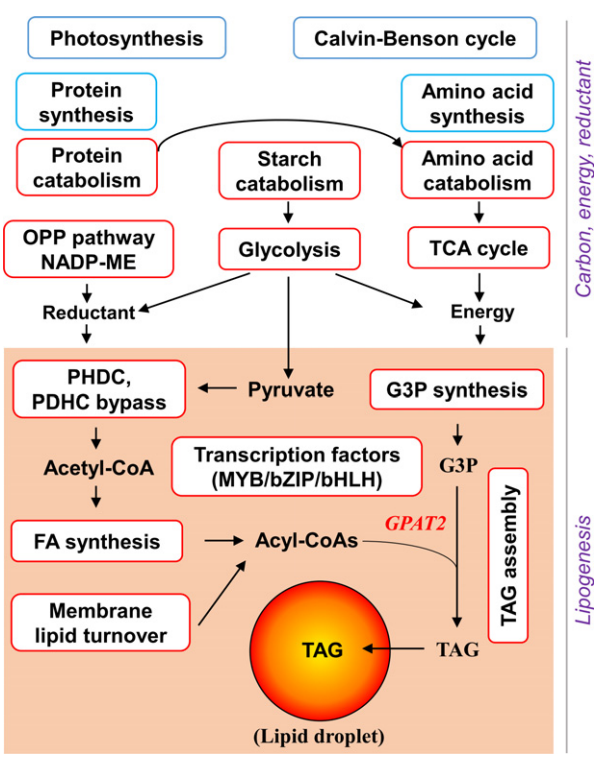

Figure 6. A mechanistic model of oleaginousness in *C. zofingiensis*. Boxes in red and blue indicated up and downregulated pathways, respectively.

EXPERIMENTAL PROCEDURES

Algal strain and growth conditions

Chromochloris zofingiensis (ATCC 30412), was from the American Type Culture Collection (ATCC, https://www.atcc.org) and maintained at 14°C on agar plates with BG-11 medium. For growth in liquid medium, the algal cells from plates were inoculated into flasks grown aerobically at 25°C for 6 days with orbital shaking (150 rpm) and continuous illumination (30 μE m^{-2} sec^{-1}). The cells were then inoculated at 10% (v/v) into 200-mL columns provided with constant illumination of 70 μE m^{-2} sec^{-1} and aeration of 1.5% CO_2 enriched air, grown to late exponential phase and used as seed cultures for subsequent experiments.

The algal cells in exponential phase (designated as 0 h of ND) were harvested by centrifugation, washed with nitrogen-free BG-11 medium three times and then re-suspended in the medium for ND treatments ($n = 3$), with constant illumination of 70 μE m^{-2} sec^{-1} and aeration of 1.5% CO_2 enriched air. Cells were sampled at 0, 12, 24, 48 and 96 h of ND for protein, starch, lipids and carotenoids, at 0 and 12 h of ND for metabolomic analysis, while at 0, 3, 6, 12 and 24 h of ND for RNA-seq.

Physiological and biochemical analyses

Fv/*Fm*, the potential quantum efficiency of PSII indicating the photosynthetic performance, was measured in dark-adapted algal cell samples (2 h) using a pulse amplitude-modulated (PAM) fluorometry (Walz, https://www.walz.com/) (Steinbrenner and Sandmann, 2006). Cell numbers were counted using a hemocytometer under a light microscope. Dry weight was determined gravimetrically following the previous procedures (Liu *et al.*, 2012a).

Algal samples were lyophilized on a freeze-drier (Labconco, https://www.labconco.com) prior to biochemical analysis. Protein was determined as described by Meijer and Wijffels (1998). Starch was determined using the Starch Assay Kit (Sigma-Aldrich, http://www.sigmaaldrich.com/) following the manual' instructions. Chlorophylls were extracted with acetone and calculated from the absorbance values at 645 and 663 nm according to Li *et al.* (2008).

Lipids were extracted with chloroform–methanol (2:1) as previously described (Liu *et al.*, 2010) and the total lipids were determined gravimetrically. For individual lipid class analysis, neutral lipids were separated on a Silica gel 60 TLC plate (Merck, https://

www.merck.com) using a mixture of hexane/tert-butylmethyl ether/acetic acid (80/20/2, by vol) as the mobile phase, while polar lipids were separated on a TLC plate using a mixture of chloroform/methanol/acetic acid/water (25/4/0.7/0.3, by vol) as the mobile phase (Liu *et al.*, 2016b). Individual lipids on TLC plate were visualized with iodine vapor, recovered and transesterified (total lipids were directly transesterified) with sulfuric acid in methanol (Liu *et al.*, 2016a). Fatty acid methyl esters were analyzed using an Agilent 7890 capillary gas chromatograph equipped with a 5975 C mass spectrometry detector and a HP-88 capillary column (60 m × 0.25 mm) (Agilent Technologies, https://www.agilent.com) as detailed by our previous procedures (Liu *et al.*, 2012b).

Metabolites were extracted with cold 80% methanol in the presence of glass beads by a mini-beadbeater (Biospec Products, https://www.biospec.com). Metabolite profiling was performed by the Metabolomics Facility at Technology Center for Protein Sciences, Tsinghua University, using a TSQ Quantiva Triple Quadrupole liquid chromatography–mass spectrometry (Thermo Scientific, San Jose, CA, USA) according to the previously described method (Le *et al.*, 2016). Metabolites were separated on a 100 × 3 mm Synergi™ Hydro-RP 100A column (Phenomenex, http://www.phenomenex.com/) at 35°C with a linear gradient from 95% mobile solvent A (10 mM tributylamine and 15 mM acetate in water) to 90% mobile solvent B (100% methanol) over a 25-min period. The flow rate was 0.3 ml min^{-1}. Positive–negative ion switching mode was used for data acquisition and the Tracefinder software was used for the identification of metabolites based on their ion transitions and retention times. Among the 145 metabolites detected, 107 had authentic standards for identification (Data S8), covering most compounds of TCA cycle, glycolysis pathway, amino acids and nucleotide metabolism. The other 38 metabolites had no authentic standards for comparison and therefore were putatively identified. Relative quantification was employed between biological conditions (0 and 12 h of ND) wherein the data from 0 h of ND serves as the reference control. Difference was considered statistically significant when the relative value showed at least a 1.5-fold change with a *P*-value less than 0.05 (*t*-test).

RNA sequencing

Total RNA under the above conditions (three biological replicates for each time point) was extracted using TRIzol reagent (Invitrogen, https://www.thermofisher.com/). The RNA quality and concentration were examined using an Agilent 2100 Bioanalyzer (Agilent Technologies) and a NanoDrop 2000C (Thermo Scientific). Total RNA (10 mg) was subjected to DNase I treatment, followed by mRNA purification with Sera-mag Magnetic Oligo(dT) Beads (Thermo Scientific). The transcriptome libraries were prepared using the NEBNext mRNA Library Prep Reagent Set (New England Biolabs, https://www.neb.com) and sequenced for 2 × 150-bp runs (paired-end) using a Illumina HiSeq 2500 sequencing system (Illumina, https://www.illumina.com) by Sangon Biotech (Shanghai) Co., Ltd, China. Reads were aligned to the *C. zofingiensis* genome (https://phytozome.jgi.doe.gov/pz/portal.html#!info?alias=Org_Czofingiensis_er) with TopHat (version 2.0.4, allowed no more than two segment mismatches) (Trapnell *et al.*, 2012). Reads mapping to more than one location were excluded. The RNA-seq data were deposited in the Gene Expression Omnibus under accession number GSE113802.

Differentially expressed gene analysis

For each of the RNA-seq data sets under each experimental condition, gene expression was measured as the numbers of aligned reads to annotated genes using Cufflinks software (version 2.0.4) and normalized to FPKM values. Genes were considered to be significantly differentially expressed if both criteria were met: their expression values showed at least a two-fold change with an FDR adjusted *P*-value less than 0.01 between control (0 h of ND) and ND conditions for at least one time point and moreover their FPKM values under at least one of the conditions were no less than 10.

The DEGs were grouped into 18 clusters based on their temporal expression patterns by the k-means clustering using the MultiExperiment Viewer 4.9 (MeV4.9; http://www.tm4.org/mev.html) with Euclidean distance. The optimal number of clusters was identified and investigated with MeV4.9 by performing a figure of merit analysis (Yeung *et al.*, 2001). The genes in each cluster were manually categorized into 12 groups according to Li *et al.* (2014).

Knockdown and overexpression of GPATs in *C. zofingiensis*

The empty vector pCZ-mPDS (Figure S11) for gene knockdown in *C. zofingiensis* was derived from pCZT1 (Liu *et al.*, 2014b). The RNAi vector construction for *GPAT1* and *GPAT2* knockdown followed the procedures described by Wei *et al.* (2017) and the resulting vectors were depicted in Figure S11. The coding sequences of *GPAT1* and *GPAT2* were PCR amplified and cloned into *Nde*I and *Bam*HI sites of pCZ-mPDS leading to the overexpression constructions of pCZ-OE-GPAT1 and pCZ-OE-GPAT2, respectively (Figure S11). The nuclear transformation of *C. zofingiensis* via electroporation followed our previously described procedures (Liu *et al.*, 2014b). Prior to transformation, the vectors were linearized by *Xba*I and purified. For overexpression, pCZ-OE-GPAT1 and pCZ-OE-GPAT2 were cut by *Xba*I and *Xho*I and each co-transformed with the linearized pCZ-mPDS. Transformants were selected on BG-11 plates with 1 μg ml^{-1} norflurazon (Sigma-Aldrich) and verified by genomic PCR (Liu *et al.*, 2014c).

Quantitative real-time PCR

Quantitative real-time PCR (qPCR) was employed to validate the RNA-seq results and determine the transcriptional levels of *GPAT*s in the knockdown and overexpression transformants. The cDNA synthesis and qPCR were performed as described by Liu *et al.* (2012b) using a 7500 Fast Real-Time PCR System (Applied Biosystems, https://www.thermofisher.com/) with SYBR Green PCR Master Mix (Invitrogen). The primers used for qPCR were listed in Table S4. The gene expression level was normalized using the housekeeping gene β-actin as the internal control, as stated in our previous studies (Liu *et al.*, 2012b, 2014b). This gene maintained stable FPKM values in response to ND (Figure S12).

ACKNOWLEDGEMENTS

This study was partially funded by grants from the National Youth Thousand Talents Program, Peking University CCUS project supported by BHP Billiton and Double-First Class Initiative of Peking University. The authors declare no conflict of interest. We thank Professor Arthur Grossman at Stanford University and Professor Jian Xu at Qingdao Institute of Bioenergy and Bioprocess Technology, Chinese Academy of Sciences for their constructive comments on the manuscript.

SUPPORTING INFORMATION

Additional Supporting Information may be found in the online version of this article.

Figure S1. Spearman correlation of transcriptomes among different biological samples.

Figure S2. Consistency between RNA-seq-based and qPCR-based transcript quantification.

Figure S3. Overview of the transcriptome dataset analysis.

Figure S4. The information of shared, ND3- and ND24-specific DEGs.

Figure S5. Time course of growth-related parameters for *C. zofingiensis* in response to ND.

Figure S6. Time course of total RNA for *C. zofingiensis* in response to ND.

Figure S7. Regulation of *de novo* fatty acid synthesis and fatty acid desaturation in *C. zofingiensis* in response to ND.

Figure S8. Fatty acid profile in *sn*-1/3 and *sn*-2 positions of TAG from *C. zofingiensis* on day 0 and day 2 of ND.

Figure S9. Regulation of membrane glycerolipid synthesis in *C. zofingiensis* in response to ND.

Figure S10. Cladogram of the DGATs from plants, fungi, algae and animals.

Figure S11. Schematic illustration of constructs for RNAi-mediated knockdown and overexpression of *GPAT*s in *C. zofingiensis* cells.

Figure S12. The time-course FPKM value of beta-actin upon ND.

Table S1. Variation of cellular content of major compounds in *C. zofingiensis* in response to ND.

Table S2. Changes of metabolites between 0 h and 12 of ND.

Table S3. General information of the transcriptomes.

Table S4. The primer sequences of selected genes used in qPCR experiments.

Table S5. RNA-seq data for genes involved in lipid metabolism.

Table S6. RNA-seq data for genes involved in photosynthesis.

Table S7. RNA-seq data for genes involved in CO_2 fixation.

Table S8. RNA-seq data for genes involved in protein metabolism.

Table S9. RNA-seq data for genes involved in amino acid metabolism.

Table S10. RNA-seq data for genes involved in purine and pyrimidine metabolism.

Table S11. RNA-seq data for genes involved in starch metabolism, glycolysis/gluconeogenesis and acyl-CoA and G3P production.

Table S12. RNA-seq data for the genes involved in transport of certain metabolites, TCA cycle and oxidative pentose phosphate pathway.

Table S13. DGAT proteins used for the construction of phylogenetic tree.

Table S14. RNA-seq data for genes encoding transcription factors.

Data S1. Genes with FPKM value no less than 1 in either of biological samples.

Data S2. Top 100 most expressed genes at 0 h of ND and 100 most upregulated and downregulated genes upon ND.

Data S3. Expression analysis of 5693 DEGs.

Data S4. Clustered DEGs with manual function curation.

Data S5. Information for shared, ND3- and ND24- specific DEGs.

Data S6. Subcellular localization prediction of proteins of selected genes.

Data S7. Pearson correlation between TFs and the genes involved in lipid metabolism and pathways for producing precursors, NADPH and energy.

Data S8. Available authentic standards for metabolite identification in the present study.

REFERENCES

Ambati, R., Phang, S.-M., Ravi, S. and Aswathanarayana, R. (2014) Astaxanthin: sources, extraction, stability, biological activities and its commercial applications—a review. *Mar. Drugs*, **12**, 128–152.

Avidan, O., Brandis, A., Rogachev, I. and Pick, U. (2015) Enhanced acetyl-CoA production is associated with increased triglyceride accumulation in the green alga *Chlorella desiccata*. *J. Exp. Bot.* **66**, 3725–3735.

Balamurugan, S., Wang, X., Wang, H.-L., An, C.-J., Li, H., Li, D.-W., Yang, W.-D., Liu, J.-S. and Li, H.-Y. (2017) Occurrence of plastidial triacylglycerol synthesis and the potential regulatory role of AGPAT in the model diatom *Phaeodactylum tricornutum*. *Biotechnol. Biofuels*, **10**, 97.

Blaby, I.K., Glaesener, A.G., Mettler, T. *et al.* (2013) Systems-level analysis of nitrogen starvation-induced modifications of carbon metabolism in a *Chlamydomonas reinhardtii* starchless mutant. *Plant Cell*, **25**, 4305–4323.

Chen, H., Zheng, Y., Zhan, J., He, C. and Wang, Q. (2017) Comparative metabolic profiling of the lipid-producing green microalga Chlorella reveals that nitrogen and carbon metabolic pathways contribute to lipid metabolism. *Biotechnol. Biofuels*, **10**, 153.

Chisti, Y. (2007) Biodiesel from microalgae. *Biotechnol. Adv.* **25**, 294–306.

Chisti, Y. (2013) Constraints to commercialization of algal fuels. *J. Biotechnol.* **167**, 201–214.

Del Campo, J.A., Rodriguez, H., Moreno, J., Vargas, M.A., Rivas, J. and Guerrero, M.G. (2004) Accumulation of astaxanthin and lutein in *Chlorella zofingiensis* (Chlorophyta). *Appl. Microbiol. Biotechnol.* **64**, 848–854.

Dinamarca, J., Levitan, O., Kumaraswamy, G.K., Lun, D.S. and Falkowski, P.G. (2017) Overexpression of a diacylglycerol acyltransferase gene in *Phaeodactylum tricornutum* directs carbon towards lipid biosynthesis. *J. Phycol.* **53**, 405–414.

Driver, T., Trivedi, D.K., McIntosh, O.A., Dean, A.P., Goodacre, R. and Pittman, J.K. (2017) Two glycerol-3-phosphate dehydrogenases from *Chlamydomonas* have distinct roles in lipid metabolism. *Plant Physiol.* **174**, 2083.

Fraser, P.D. and Bramley, P.M. (2004) The biosynthesis and nutritional uses of carotenoids. *Prog. Lipid Res.* **43**, 228–265.

Gargouri, M., Park, J.-J., Holguin, F.O., Kim, M.-J., Wang, H., Deshpande, R.R., Shachar-Hill, Y., Hicks, L.M. and Gang, D.R. (2015) Identification of regulatory network hubs that control lipid metabolism in *Chlamydomonas reinhardtii*. *J. Exp. Bot.* **66**, 4551–4566.

Goodenough, U., Blaby, I., Casero, D. *et al.* (2014) The path to triacylglyceride obesity in the *sta6* strain of *Chlamydomonas reinhardtii*. *Eukaryot. Cell*, **13**, 591–613.

Hu, Q., Sommerfeld, M., Jarvis, E., Ghirardi, M., Posewitz, M., Seibert, M. and Darzins, A. (2008) Microalgal triacylglycerols as feedstocks for biofuel production: perspectives and advances. *Plant J.* **54**, 621–639.

Ip, P.F., Wong, K.H. and Chen, F. (2004) Enhanced production of astaxanthin by the green microalga *Chlorella zofingiensis* in mixotrophic culture. *Process Biochem.* **39**, 1761–1766.

Iskandarov, U., Sitnik, S., Shtaida, N., Didi-Cohen, S., Leu, S., Khozin-Goldberg, I., Cohen, Z. and Boussiba, S. (2016) Cloning and characterization of a GPAT-like gene from the microalga *Lobosphaera incisa* (Trebouxiophyceae): overexpression in *Chlamydomonas reinhardtii* enhances TAG production. *J. Appl. Phycol.* **28**, 907–919.

Iwai, M., Ikeda, K., Shimojima, M. and Ohta, H. (2014) Enhancement of extraplastidic oil synthesis in *Chlamydomonas reinhardtii* using a type-2 diacylglycerol acyltransferase with a phosphorus starvation-inducible promoter. *Plant Biotechnol. J.* **12**, 808–819.

Jaeger, D., Winkler, A., Mussgnug, J.H., Kalinowski, J., Goesmann, A. and Kruse, O. (2017) Time-resolved transcriptome analysis and lipid pathway reconstruction of the oleaginous green microalga *Monoraphidium neglectum* reveal a model for triacylglycerol and lipid hyperaccumulation. *Biotechnol. Biofuels*, **10**, 197.

Kang, N.K., Jeon, S., Kwon, S., Koh, H.G., Shin, S.-E., Lee, B., Choi, G.-G., Yang, J.-W., Jeong, B.-R. and Chang, Y.K. (2015) Effects of overexpression of a bHLH transcription factor on biomass and lipid production in *Nannochloropsis salina*. *Biotechnol. Biofuels*, **8**, 1–13.

Kang, N.K., Kim, E.K., Kim, Y.U., Lee, B., Jeong, W.-J., Jeong, B.-R. and Chang, Y.K. (2017) Increased lipid production by heterologous expression of AtWRI1 transcription factor in *Nannochloropsis salina*. *Biotechnol. Biofuels*, **10**, 231.

Kim, Y., Terng, E.L., Riekhof, W.R., Cahoon, E.B. and Cerutti, H. (2018) Endoplasmic reticulum acyltransferase with prokaryotic substrate preference contributes to triacylglycerol assembly in *Chlamydomonas*. *Proc. Natl. Aca. Sci. USA*, **115**, 1652–1657.

Klein, U. (1986) Compartmentation of glycolysis and of the oxidative pentose-phosphate pathway in *Chlamydomonas reinhardtii*. *Planta*, **167**, 81–86.

Kong, F., Liang, Y., Legeret, B., Beyly-Adriano, A., Blangy, S., Haslam, R.P., Napier, J.A., Beisson, F., Peltier, G. and Li-Beisson, Y. (2017) *Chlamydomonas* carries out fatty acid beta-oxidation in ancestral peroxisomes using a bona fide acyl-CoA oxidase. *Plant J.* **90**, 358–371.

Kong, F., Romero, I.T., Warakanont, J. and Li-Beisson, Y. (2018) Lipid catabolism in microalgae. *New Phytol.* **218**, 1340–1348.

Körbes, A.P., Kulcheski, F.R., Margis, R., Margis-Pinheiro, M. and Turchetto-Zolet, A.C. (2016) Molecular evolution of the lysophosphatidic acid acyltransferase (LPAAT) gene family. *Mol. Phylogenet. Evol.* **96**, 55–69.

Kwon, S., Kang, N.K., Koh, H.G., Shin, S.-E., Lee, B., Jeong, B.-R. and Chang, Y.K. (2018) Enhancement of biomass and lipid productivity by overexpression of a bZIP transcription factor in *Nannochloropsis salina*. *Biotechnol. Bioeng.* **115**, 331–340.

Le, L., Jiang, B., Wan, W., Zhai, W., Xu, L., Hu, K. and Xiao, P. (2016) Metabolomics reveals the protective of Dihydromyricetin on glucose homeostasis by enhancing insulin sensitivity. *Sci. Rep.* **6**, 36184.

Lenka, S.K., Carbonaro, N., Park, R., Miller, S.M., Thorpe, I. and Li, Y. (2016) Current advances in molecular, biochemical, and computational modeling analysis of microalgal triacylglycerol biosynthesis. *Biotechnol. Adv.* **34**, 1046–1063.

Li, Y., Horsman, M., Wang, B., Wu, N. and Lan, C. (2008) Effects of nitrogen sources on cell growth and lipid accumulation of green alga *Neochloris oleoabundans*. *Appl. Microbiol. Biotechnol.* **81**, 629–636.

Li, Y., Han, D., Hu, G., Dauvillee, D., Sommerfeld, M., Ball, S. and Hu, Q. (2010) *Chlamydomonas* starchless mutant defective in ADP-glucose pyrophosphorylase hyper-accumulates triacylglycerol. *Metab. Eng.* **12**, 387–391.

Li, X., Moellering, E.R., Liu, B., Johnny, C., Fedewa, M., Sears, B.B., Kuo, M.-H. and Benning, C. (2012a) A galactoglycerolipid lipase is required for triacylglycerol accumulation and survival following nitrogen deprivation in *Chlamydomonas reinhardtii*. *Plant Cell*, **24**, 4670–4686.

Li, X., Benning, C. and Kuo, M.-H. (2012b) Rapid triacylglycerol turnover in *chlamydomonas reinhardtii* requires a lipase with broad substrate specificity. *Eukaryot. Cell*, **11**, 1451–1462.

Li, J., Han, D., Wang, D. *et al.* (2014) Choreography of transcriptomes and lipidomes of *Nannochloropsis* reveals the mechanisms of oil synthesis in microalgae. *Plant Cell*, **26**, 1645–1665.

Li-Beisson, Y., Beisson, F. and Riekhof, W. (2015) Metabolism of acyl-lipids in *Chlamydomonas reinhardtii*. *Plant J.* **82**, 504–522.

Linka, N. and Weber, A.P.M. (2010) Intracellular metabolite transporters in plants. *Mol. Plant*, **3**, 21–53.

Liu, J., Huang, J., Fan, K.W., Jiang, Y., Zhong, Y., Sun, Z. and Chen, F. (2010) Production potential of *Chlorella zofingienesis* as a feedstock for biodiesel. *Bioresour. Technol.* **101**, 8658–8663.

Liu, J., Huang, J., Sun, Z., Zhong, Y., Jiang, Y. and Chen, F. (2011) Differential lipid and fatty acid profiles of photoautotrophic and heterotrophic *Chlorella zofingiensis*: assessment of algal oils for biodiesel production. *Bioresour. Technol.* **102**, 106–110.

Liu, J., Huang, J., Jiang, Y. and Chen, F. (2012a) Molasses-based growth and production of oil and astaxanthin by *Chlorella zofingiensis*. *Bioresour. Technol.* **107**, 393–398.

Liu, J., Sun, Z., Zhong, Y., Huang, J., Hu, Q. and Chen, F. (2012b) Stearoyl-acyl carrier protein desaturase gene from the oleaginous microalga *Chlorella zofingiensis*: cloning, characterization and transcriptional analysis. *Planta*, **236**, 1665–1676.

Liu, J., Sun, Z., Zhong, Y., Gerken, H., Huang, J. and Chen, F. (2013) Utilization of cane molasses towards cost-saving astaxanthin production by a *Chlorella zofingiensis* mutant. *J. Appl. Phycol.* **25**, 1447–1456.

Liu, J., Sun, Z., Gerken, H., Liu, Z., Jiang, Y. and Chen, F. (2014a) *Chlorella zofingiensis* as an alternative microalgal producer of astaxanthin: biology and industrial potential. *Mar. Drugs*, **12**, 3487–3515.

Liu, J., Sun, Z., Gerken, H., Huang, J., Jiang, Y. and Chen, F. (2014b) Genetic engineering of the green alga *Chlorella zofingiensis*: a modified norflurazon-resistant phytoene desaturase gene as a dominant selectable marker. *Appl. Microbiol. Biotechnol.* **98**, 5069–5079.

Liu, J., Gerken, H. and Li, Y. (2014c) Single-tube colony PCR for DNA amplification and transformant screening of oleaginous microalgae. *J. Appl. Phycol.* **26**, 1719–1726.

Liu, J., Mao, X., Zhou, W. and Guarnieri, M.T. (2016a) Simultaneous production of triacylglycerol and high-value carotenoids by the astaxanthin-producing oleaginous green microalga *Chlorella zofingiensis*. *Bioresour. Technol.* **214**, 319–327.

Liu, J., Han, D., Yoon, K., Hu, Q. and Li, Y. (2016b) Characterization of type 2 diacylglycerol acyltransferases in *Chlamydomonas reinhardtii* reveals their distinct substrate specificities and functions in triacylglycerol biosynthesis. *Plant J.* **86**, 3–19.

López García de Lomana, A., Schäuble, S., Valenzuela, J. *et al.* (2015) Transcriptional program for nitrogen starvation-induced lipid accumulation in *Chlamydomonas reinhardtii*. *Biotechnol. Biofuels*, **8**, 1–18.

Ma, X., Liu, J., Liu, B., Chen, T., Yang, B. and Chen, F. (2016) Physiological and biochemical changes reveal stress-associated photosynthetic carbon partitioning into triacylglycerol in the oleaginous marine alga *Nannochloropsis oculata*. *Algal Res.* **16**, 28–35.

Mao, X., Wu, T., Kou, Y., Shi, Y., Zhang, Y. and Liu, J. (2019) Characterization of type I and type II diacylglycerol acyltransferases from the emerging model alga *Chlorella zofingiensis* reveals their functional complementarity and engineering potential. *Biotechnol. Biofuels*, **12**, 28.

Meijer, E.A. and Wijffels, R.H. (1998) Development of a fast, reproducible and effective method for the extraction and quantification of proteins of micro-algae. *Biotechnol. Tech.* **12**, 353–358.

Merchant, S.S., Kropat, J., Liu, B., Shaw, J. and Warakanont, J. (2012) TAG, You're it! *Chlamydomonas* as a reference organism for understanding algal triacylglycerol accumulation. *Curr. Opin. Biotechnol.* **23**, 352–363.

Miller, R., Wu, G., Deshpande, R.R. *et al.* (2010) Changes in transcript abundance in *Chlamydomonas reinhardtii* following nitrogen deprivation predict diversion of metabolism. *Plant Physiol.* **154**, 1737–1752.

Moellering, E.R. and Benning, C. (2010) RNA interference silencing of a major lipid droplet protein affects lipid droplet size in *Chlamydomonas reinhardtii*. *Eukaryot. Cell*, **9**, 97–106.

Mulders, K.J.M., Janssen, J.H., Martens, D.E., Wijffels, R.H. and Lamers, P.P. (2014) Effect of biomass concentration on secondary carotenoids and triacylglycerol (TAG) accumulation in nitrogen-depleted *Chlorella zofingiensis*. *Algal Res.* **6**, 8–16.

Niu, Y.-F., Wang, X., Hu, D.-X., Balamurugan, S., Li, D.-W., Yang, W.-D., Liu, J.-S. and Li, H.-Y. (2016) Molecular characterization of a glycerol-3-phosphate acyltransferase reveals key features essential for triacylglycerol production in *Phaeodactylum tricornutum*. *Biotechnol. Biofuels*, **9**, 60.

Ohlrogge, J. and Browse, J. (1995) Lipid biosynthesis. *Plant Cell*, **7**, 957–970.

Park, J.-J., Wang, H., Gargouri, M., Deshpande, R.R., Skepper, J.N., Holguin, F.O., Juergens, M.T., Shachar-Hill, Y., Hicks, L.M. and Gang, D.R. (2015) The response of *Chlamydomonas reinhardtii* to nitrogen deprivation: a systems biology analysis. *Plant J.* **81**, 611–624.

Raheem, A., Prinsen, P., Vuppaladadiyam, A.K., Zhao, M. and Luque, R. (2018) A review on sustainable microalgae based biofuel and bioenergy production: recent developments. *J. Clean. Prod.* **181**, 42–59.

Ratledge, C. (2014) The role of malic enzyme as the provider of NADPH in oleaginous microorganisms: a reappraisal and unsolved problems. *Biotechnol. Lett.* **36**, 1557–1568.

Rawsthorne, S. (2002) Carbon flux and fatty acid synthesis in plants. *Prog. Lipid Res.* **41**, 182–196.

Rengel, R., Smith, R.T., Haslam, R.P., Sayanova, O., Vila, M. and León, R. (2018) Overexpression of acetyl-CoA synthetase (ACS) enhances the biosynthesis of neutral lipids and starch in the green microalga *Chlamydomonas reinhardtii*. *Algal Res.* **31**, 183–193.

Rodionova, M.V., Poudyal, R.S., Tiwari, I., Voloshin, R.A., Zharmukhamedov, S.K., Nam, H.G., Zayadan, B.K., Bruce, B.D., Hou, H.J.M. and Allakhverdiev, S.I. (2017) Biofuel production: challenges and opportunities. *Int. J. Hydrogen Energy*, **42**, 8450–8461.

Roth, M.S., Cokus, S.J., Gallaher, S.D. *et al.* (2017) Chromosome-level genome assembly and transcriptome of the green alga *Chromochloris zofingiensis* illuminates astaxanthin production. *Proc. Natl Acad. Sci. USA*, **114**, 4296–4305.

Sanjaya, Miller, R., Durrett, T.P. *et al.* (2013) Altered lipid composition and enhanced nutritional value of Arabidopsis leaves following introduction of an algal diacylglycerol acyltransferase 2. *Plant Cell* **25**, 677–693.

Steinbrenner, J. and Sandmann, G. (2006) Transformation of the green alga *Haematococcus pluvialis* with a phytoene desaturase for accelerated astaxanthin biosynthesis. *Appl. Environ. Microbiol.* **72**, 7477–7484.

Sun, N., Wang, Y., Li, Y.-T., Huang, J.-C. and Chen, F. (2008) Sugar-based growth, astaxanthin accumulation and carotenogenic transcription of heterotrophic *Chlorella zofingiensis* (Chlorophyta). *Process Biochem.* **43**, 1288–1292.

Trapnell, C., Roberts, A., Goff, L., Pertea, G., Kim, D., Kelley, D.R., Pimentel, H., Salzberg, S.L., Rinn, J.L. and Pachter, L. (2012) Differential gene and transcript expression analysis of RNA-seq experiments with TopHat and Cufflinks. *Nat. Protoc.* **7**, 562–578.

Trentacoste, E.M., Shrestha, R.P., Smith, S.R., Glé, C., Hartmann, A.C., Hildebrand, M. and Gerwick, W.H. (2013) Metabolic engineering of lipid catabolism increases microalgal lipid accumulation without compromising growth. *Proc. Natl Acad. Sci. USA*, **110**, 19748–19753.

Wei, H., Shi, Y., Ma, X., Pan, Y., Hu, H., Li, Y., Luo, M., Gerken, H. and Liu, J. (2017) A type-I diacylglycerol acyltransferase modulates triacylglycerol biosynthesis and fatty acid composition in the oleaginous microalga. Nannochloropsis oceanica. *Biotechnol. Biofuels*, **10**, 174.

Wijffels, R.H. and Barbosa, M.J. (2010) An outlook on microalgal biofuels. *Science*, **329**, 796–799.

Xin, Y., Lu, Y., Lee, Y.-Y. *et al.* (2017) Producing designer oils in industrial microalgae by rational modulation of co-evolving type-2 diacylglycerol acyltransferases. *Mol. Plant*, **10**, 1523–1539.

Xue, J., Niu, Y.-F., Huang, T., Yang, W.-D., Liu, J.-S. and Li, H.-Y. (2015) Genetic improvement of the microalga *Phaeodactylum tricornutum* for boosting neutral lipid accumulation. *Metab. Eng.* **27**, 1–9.

Xue, J., Balamurugan, S., Li, D.W., Liu, Y.H., Zeng, H., Wang, L., Yang, W.D., Liu, J.S. and Li, H.Y. (2017) Glucose-6-phosphate dehydrogenase as a target for highly efficient fatty acid biosynthesis in microalgae by enhancing NADPH supply. *Metab. Eng.* **41**, 212–221.

Yamaoka, Y., Achard, D., Jang, S. *et al.* (2016) Identification of a *Chlamydomonas* plastidial 2-lysophosphatidic acid acyltransferase and its use to engineer microalgae with increased oil content. *Plant Biotechnol. J.* **14**, 2158–2167.

Yan, J., Cheng, R., Lin, X., You, S., Li, K., Rong, H. and Ma, Y. (2013) Overexpression of acetyl-CoA synthetase increased the biomass and fatty acid proportion in microalga *Schizochytrium*. *Appl. Microbiol. Biotechnol.* **97**, 1933–1939.

Yao, Y., Lu, Y., Peng, K.-T., Huang, T., Niu, Y.-F., Xie, W.-H., Yang, W.-D., Liu, J.-S. and Li, H.-Y. (2014) Glycerol and neutral lipid production in the oleaginous marine diatom *Phaeodactylum tricornutum* promoted by overexpression of glycerol-3-phosphate dehydrogenase. *Biotechnol. Biofuels*, **7**, 110.

Yeung, K.Y., Haynor, D.R. and Ruzzo, W.L. (2001) Validating clustering for gene expression data. *Bioinformatics*, **17**, 309–318.

Yoon, K., Han, D., Li, Y., Sommerfeld, M. and Hu, Q. (2012) Phospholipid:diacylglycerol acyltransferase is a multifunctional enzyme involved in membrane lipid turnover and degradation while synthesizing triacylglycerol in the unicellular green microalga *Chlamydomonas reinhardtii*. *Plant Cell*, **24**, 3708–3724.

Zhang, J., Hao, Q., Bai, L. *et al.* (2014) Overexpression of the soybean transcription factor GmDof4 significantly enhances the lipid content of *Chlorella ellipsoidea*. *Biotechnol. Biofuels*, **7**, 1–16.

Zhao, L., Tang, X., Luan, X., Chen, H., Chen, Y.Q., Chen, W., Song, Y. and Ratledge, C. (2015) Role of pentose phosphate pathway in lipid accumulation of oleaginous fungus *Mucor circinelloides*. *RSC Adv.* **5**, 97658–97664.

Zhou, W., Wang, J., Chen, P., Ji, C., Kang, Q., Lu, B., Li, K., Liu, J. and Ruan, R. (2017) Bio-mitigation of carbon dioxide using microalgal systems: advances and perspectives. *Renew. Sust. Energ. Rev.* **76**, 1163–1175.

Zhu, S., Huang, W., Xu, J., Wang, Z., Xu, J. and Yuan, Z. (2014) Metabolic changes of starch and lipid triggered by nitrogen starvation in the microalga *Chlorella zofingiensis*. *Bioresour. Technol.* **152**, 292–298.

Zienkiewicz, K., Zienkiewicz, A., Poliner, E., Du, Z.-Y., Vollheyde, K., Herrfurth, C., Marmon, S., Farré, E.M., Feussner, I. and Benning, C. (2017) *Nannochloropsis*, a rich source of diacylglycerol acyltransferases for engineering of triacylglycerol content in different hosts. *Biotechnol. Biofuels*, **10**, 8.

